

RESEARCH

Open Access



Sex-specific DNA methylation differences in Alzheimer's disease pathology

Lanyu Zhang¹, Juan I. Young^{2,3}, Lissette Gomez³, Tiago C. Silva¹, Michael A. Schmidt^{2,3}, Jesse Cai⁴, Xi Chen^{1,5}, Eden R. Martin^{2,3} and Lily Wang^{1,2,3,5*}

Abstract

Sex is an important factor that contributes to the clinical and biological heterogeneities in Alzheimer's disease (AD), but the regulatory mechanisms underlying sex disparity in AD are still not well understood. DNA methylation is an important epigenetic modification that regulates gene transcription and is known to be involved in AD. We performed the first large-scale sex-specific meta-analysis of DNA methylation differences in AD neuropathology, by re-analyzing four recent epigenome-wide association studies totaling more than 1000 postmortem prefrontal cortex brain samples using a uniform analytical pipeline. For each cohort, we employed two complementary analytical strategies, a sex-stratified analysis that examined methylation-Braak stage associations in male and female samples separately, and a sex-by-Braak stage interaction analysis that compared the magnitude of these associations between different sexes. Our analysis uncovered 14 novel CpGs, mapped to genes such as *TMEM39A* and *TNXB* that are associated with the AD Braak stage in a sex-specific manner. *TMEM39A* is known to be involved in inflammation, dysregulated type I interferon responses, and other immune processes. *TNXB* encodes tenascin proteins, which are extracellular matrix glycoproteins demonstrated to modulate synaptic plasticity in the brain. Moreover, for many previously implicated genes in AD neuropathology, such as *MBP* and *AZU1*, our analysis provided the new insights that they were predominately driven by effects in only one sex. These sex-specific DNA methylation differences were enriched in divergent biological processes such as integrin activation in females and complement activation in males. Our study implicated multiple new loci and biological processes that affected AD neuropathology in a sex-specific manner.

Keywords: Alzheimer's disease, Sex-specific, DNA methylation, Epigenome-wide association study

Introduction

Late-onset Alzheimer's disease (LOAD) is the most common cause of dementia. With the aging population in the U.S., Alzheimer's disease (AD) has become a major public health concern and one of the most financially costly diseases [1]. Almost two-thirds of AD patients in the U.S. are women [2]. After diagnosis, women also progress faster with more rapid cognitive and functional declines

[3–8]. On the other hand, it has also been reported men with AD have an increased risk for death [9–11]. However, the molecular mechanisms underlying these observed disparities in AD are still not well understood. Previous studies have shown that epigenetics is an important contributor to the sex differences in brain functions and vulnerability to diseases [12–16]. Among epigenetic modifications, DNA methylation profiles differ significantly between males and females at many loci in adult brains [17]. Importantly, alterations of DNA methylation levels have also been implicated in multiple neurological disorders including AD [18–22].

*Correspondence: lily.wang@gmail.com

¹ Division of Biostatistics, Department of Public Health Sciences, University of Miami, Miller School of Medicine, Miami, FL 33136, USA
Full list of author information is available at the end of the article



However, thus far, a comprehensive characterization for the contribution of sex to DNA methylation differences in AD neuropathology has not been performed. In the identification of sex-specific effects, statistical power is a major challenge [23]. Stratifying by sex reduces the sample size of both groups. Also, comparing methylation to disease associations between the sexes by testing the interaction effect would require a much larger sample size than detecting the main effect with the same magnitude [24]. To address these challenges, we performed a comprehensive meta-analysis of more than 1000 post-mortem brain prefrontal cortex (PFC) samples, collected from four recent AD epigenome-wide association studies [18–21], to identify the most consistent DNA methylation differences affected by AD neuropathology in a sex-specific manner. Within each cohort, to identify sex-specific differences in AD neuropathology, we employed two complementary approaches, a sex-stratified analysis that examined methylation-Braak stage associations in female and male samples separately, and a sex-by-Braak stage interaction analysis that compared the magnitude of these associations between different sexes. As sex is a strong factor in driving inter-personal variabilities in AD, the results of this study are particularly relevant for precision medicine.

Methods

Study cohorts

Our meta-analysis included 1,030 prefrontal cortex brain samples (642 female samples and 388 male samples) from four independent cohorts (Additional file 2: Table S1), previously described in the ROSMAP [18], Mt. Sinai [20], London [19], and Gasparoni [21] DNA methylation studies.

Pre-processing of DNA methylation data

All the samples in this study were measured using the Infinium HumanMethylation450 BeadChip. Additional file 2: Table S2 shows the number of CpGs and samples removed at each quality control step. Quality control for CpG probes included removing probes with detection P-value < 0.01 in all samples of a cohort using the minfi R package, removing the 2623 CpGs associated with cigarette smoking identified in Joehanes et al. [25] (at P-value < 1×10^{-7} threshold), and removing CpGs having a single nucleotide polymorphism (SNP) with minor allele frequency (MAF) ≥ 0.01 present in the last 5 base pairs of the probe using the DMRcate R package (with function `rmSNPandCH` and option `dist=5`, `mafcut=0.01`). For the quality control of samples, we removed samples with low bisulfite conversion efficiency (i.e., < 88%) or detected as outliers in principal component analysis (PCA). More specifically, PCA was

performed using the 50,000 most variable CpGs for each cohort. Samples that were within ± 3 standard deviations from the means of PC1 and PC2 were selected to be included in the final sample set. The quality-controlled methylation datasets were next subjected to the QN.BMIQ normalization procedure as recommended by a recent systematic study of different normalization methods [26]. More specifically, we first applied quantile normalization as implemented in the lumi R package to remove systematic effects between samples. Next, we applied the β -mixture quantile normalization (BMIQ) procedure [27] as implemented in the wateRmelon R package [28] to normalize beta values of type 1 and type 2 design probes within the Illumina arrays. Finally, to remove batch effects, we applied the linear model methylation M value ~ methylation slide to M values of each CpG. The methylation residuals from these linear models were then used for subsequent analysis.

Single cohort analysis

To identify sex-specific DNA methylation differences in AD neuropathology, we performed both a sex-stratified analysis and a sex-by-Braak stage interaction analysis for each of the four brain sample cohorts. In the sex-stratified analysis, we tested methylation-Braak stage associations in female and male samples separately. In sex-by-Braak stage interaction analysis, we analyzed both female and male samples simultaneously and compared slopes for methylation-Braak stage associations in females and males.

More specifically, in the sex-stratified analysis, for each CpG, we applied the model methylation residuals ~ age at death + Braak stage + estimated neuron proportions to female samples and male samples separately, where methylation residuals were obtained in “Pre-processing of DNA methylation data” described above. Here, the neuron proportion for each sample was estimated using the CETS R package [29], an R software that quantifies neuronal proportions from DNA methylation data using cell epigenotype specific (CETS) marks. In sex-by-Braak stage interaction analysis, for each CpG, we applied the model methylation residuals ~ age at death + sex + Braak stage + sex * Braak stage + sex * age at death + estimated neuron proportions to samples including both sexes.

For the analysis of differentially methylated regions (DMRs), we used the coMethDMR R package [30] to analyze 40,010 pre-defined genomic regions on the Illumina 450 k arrays and identify co-methylated DMRs associated with Braak stage. The pre-defined genomic regions are regions on the Illumina array covered with clusters of contiguous CpGs where the maximum separation between any two consecutive probes is 200 base pairs. First, coMethDMR selects *co-methylated regions* within

these pre-defined contiguous genomic regions. Next, we summarized methylation M values within these co-methylated regions using medians and tested them against the AD Braak stage. The same linear models described for the analysis of CpGs were then applied to the median value of each DMR. We considered CpGs (or DMRs) with a false discovery rate (FDR) less than 0.05 in female samples or male samples to be significant.

Inflation assessment and correction

For genome-wide discoveries to be valid, the false positive rate of the study should be properly controlled. Because systematic inflation of test statistics can lead to an increase in the number of false-positive results, traditionally genomic inflation factor [31] is typically used to quantify the amount of inflation in genome-wide association studies (GWAS) of genetic variants. However, as shown by simulation studies [32], real datasets [32], and theory [31], the conventional genomic inflation factor (λ or λ used interchangeably below) is dependent on the expected number of true associations. Because in a typical epigenome-wide association study (EWAS), it is expected that small effects from many CpGs might be associated with the phenotype, the genomic inflation factor would overestimate actual test-statistic inflation. To estimate genomic inflations more accurately in EWAS, Itonson et al. [32] developed a Bayesian method that estimates inflation in EWAS based on empirical null distributions, which is implemented in the Bioconductor package *bacon*.

In this study, to assess inflation of the test statistics, we used quantile–quantile (QQ) plots and estimated genomic inflation factors using both the conventional approach and the *bacon* method [32] (Additional file 1: Fig. S1). The *bacon* method was also used to obtain inflation-corrected effect sizes, standard errors, and P-values for each cohort, which were then combined by inverse-variance weighted meta-analysis models using R package *meta*.

Meta-analysis

The evidence for heterogeneity of study effects was tested using Cochran's Q statistic [33]. The inverse-variance weighted fixed effects model was first applied to synthesize statistical significance from individual cohorts. Even though the fixed effects model for meta-analysis does not require the assumption of homogeneity [34], for the CpGs (or genomic regions) with nominal evidence for heterogeneity (nominal $P_{\text{heterogeneity}} < 0.05$), we also applied random effects meta-analysis [35] and assigned final meta-analysis P-value based on the random effects model. For each CpG (and for each genomic region), we used the R package *meta* to obtain Braak stage effect in

female samples and male samples separately in sex-stratified analysis, as well as meta-analysis P-values for sex-by-Braak stage interaction.

Identifying sex-specific differences

In the sex-stratified analysis, we selected significant CpGs (or genomic regions) with $FDR < 0.05$ in female samples or male samples separately. In sex-by-Braak stage interaction analysis, because the standard error of interaction effect $\text{sex} \times \text{Braak stage}$ is typically much larger than those for main Braak stage effects, the conventional approach for controlling false discovery rate often results in low power for discovering interaction effects [36]. Therefore, we used a stagewise analysis approach, previously proposed by van de Berge et al. (2017) [36], to help improve power in high-throughput experiments where multiple hypotheses are tested for each gene. More specifically, in the *screening step*, for each CpG (or genomic region), we tested the global null hypothesis that there is methylation-Braak stage association in either male or female samples. Next, in the *confirmation step*, we considered three individual null hypotheses for each CpG (or DMR): (a) there is no methylation-Braak stage association in male samples, (b) there is no methylation-Braak stage association in female samples, and (c) the methylation-Braak stage associations in male samples and female samples are the same. For the CpGs (or genomic region) selected in the screening step, these three individual hypotheses were then tested while controlling family-wise error rate (FWER) as described in van de Berge et al. (2017)[36].

The stagewise analysis described above was implemented using the *stageR* package to identify CpGs (or genomic regions) with significant differential methylation–Braak stage associations in females and males. In the screening step, we considered meta-analysis P-values for the Braak stage in female samples and male samples ($p_{\text{meta.female}}$, $p_{\text{meta.male}}$), and used the minimum of these two meta-analysis P-values to represent each CpG (or genomic region). In the confirmation step, the parameter $p_{\text{Confirmation}}$ was defined using three P-values for each CpG (or genomic region): $p_{\text{meta.female}}$, $p_{\text{meta.male}}$, and $p_{\text{meta.interaction}}$ (meta-analysis P-value for $\text{sex} \times \text{Braak stage}$).

Enrichment and pathway analysis

The probes on the Illumina 450k array are annotated according to their locations with respect to genes (TSS1500, TSS200, 5'UTR, 1stExon, gene body, 3'UTR, intergenic) or CpG islands (island, shore, shelf, open sea). To understand the genomic context of sex-specific DNA methylation differences in AD neuropathology, we compared the FDR significant methylation differences from

sex-stratified analysis with different types of genomic features. As Braak-associated methylation differences can occur at both significant individual CpGs and significant DMRs, we considered the CpGs located at significant individual CpGs or within significant DMRs jointly in this analysis, by testing their over- and under-representation in different types of genomic features using Fisher's exact test. More specifically, the proportion of significant CpGs mapped to a particular type of genomic feature (e.g., CpG islands) (foreground) was compared to the proportion of CpGs on the array that mapped to the same type of genomic feature (background).

Also, we used Fisher's test to assess enrichment of significant CpGs and DMRs in different chromatin states by comparing with the 15-chromatin state data for bulk PFC tissue samples (E073) from the Roadmap Epigenomics Project [37]. Using combinations of histone modification marks, ChromHMM [38] was previously used to annotate segments of the genome with different chromatin states (repressed, poised, and active promoters, strong and weak enhancers, putative insulators, transcribed regions, and large-scale repressed and inactive domains), which were shown to vary across sex, tissue type, and developmental age [39]. Similarly, we tested enrichment of significant CpGs and DMRs in binding sites of transcription factors and chromatin proteins from the ENCODE project [40] and CODEX database [41] using Locus Overlap Analysis as implemented in the LOLA R package [42].

Finally, we performed pathway analysis by comparing the genes with significant DNA methylation differences in AD neuropathology (identified in sex-stratified analysis) with the canonical pathways and biological process GO terms in MSigDB using Gene Set Enrichment Analysis (GSEA) [43]. First, we linked each CpG and each predefined genomic region tested in DMR analysis to genes by annotating them using the GREAT (Genomic Regions Enrichment of Annotations Tool) software, which associates genomic regions to target genes. With the default "Basal plus method", GREAT links each gene to a regulatory region consisting of a basal domain that extends 5 kb upstream and 1 kb downstream from its transcription start site, and an extension up to the basal regulatory region of the nearest upstream and downstream genes within 1 Mb [44]. Next, we represented each gene by the smallest P-value if there are multiple CpGs or genomic regions associated with them. To remove selection bias due to different numbers of CpGs or genomic regions associated with each gene (i.e., the smallest P-value for a gene with many CpGs or genomic regions linked to it is likely to be smaller than the smallest P-value for a gene with only a few linked CpGs or genomic regions), we next fit a generalized additive model [45] using the R package

mgcv: $Y_i \sim f(n.links_i)$ where Y_i is negative log (base 10) transformation of the smallest P-value for gene i in the analysis of female samples (or male samples), $n.links_i$ is the number of CpGs or genomic regions linked to gene i , and f is a penalized spline function. We assumed gamma distribution for Y_i , as under the null hypothesis of no association, Y_i follows the chi-square distribution (a special case of gamma distribution). The residuals from this model were estimated and used to generate a ranked gene list, which was then used as input for GSEA (in pre-ranked mode) to identify canonical pathways and gene ontology terms (MSigDB C2:CP and C5:BP collections of gene sets) enriched with significant methylation differences in female samples and male samples separately.

Integrative methylation and gene expression analysis

To systematically evaluate transcriptional differences near the observed sex-specific DNA methylation differences, we next performed integrative methylation—gene expression analysis using data on 333 female samples and 196 male samples from the ROSMAP study with matched DNA methylation and RNA-seq gene expression profiles measured on the prefrontal cortex. To this end, normalized FPKM (Fragments Per Kilobase of transcript per Million mapped reads) gene expression values for the ROSMAP study were downloaded from the AMP-AD Knowledge Portal (Synapse ID: syn3388564).

First, we linked significant CpGs (or DMRs) to nearby genes using GREAT [44], which associates genomic regions to target genes. Next, we removed confounding effects in DNA methylation data by fitting the model $M \text{ value} \sim \text{neuron.proportion} + \text{batch} + \text{sample.plate} + \text{ageAtDeath}$ and extracting residuals from this model; these are the *ROSMAP methylation residuals*. Similarly, we also removed potential confounding effects in RNA-seq data by fitting model $\log_2(\text{normalized FPKM values} + 1) \sim \text{ageAtDeath} + \text{markers for cell types}$. The last term, "markers for cell types," included multiple covariate variables to adjust for the multiple types of cells in the brain samples. More specifically, we estimated expression levels of genes that are specific for the five main cell types present in the CNS: ENO2 for neurons, GFAP for astrocytes, CD68 for microglia, OLIG2 for oligodendrocytes, and CD34 for endothelial cells, and included these as variables in the above linear regression model, as in previous large study of AD samples [18]. The residuals extracted from this model are the *ROSMAP gene expression residuals*.

Finally, for each gene expression and CpG (or DMR) pair, we then tested the association between gene expression residuals and methylation residuals using a linear model: *ROSMAP gene expression residuals* \sim *ROSMAP methylation residuals* + Braak stage. For significant

DMRs, this analysis was repeated, except that methylation M value was replaced with median methylation M value from multiple CpGs in the DMR.

Sex-specific mQTL analysis

To identify methylation quantitative trait loci (mQTLs) for the significant DMRs and CpGs, we tested associations between the methylation levels with nearby SNPs, using the ROSMAP study dataset, which had matched genotype data and DNA methylation data for 434 female samples and 254 male samples. The ROSMAP genotype data was downloaded from AMP-AD (syn3157325) and imputed to the Haplotype Reference Consortium r1.1 reference panel [46]. There were two batches of genotype data, measured by Affymetrix GeneChip 6.0 (Affymetrix, Inc, Santa Clara, CA, USA) and Illumina HumanOmni-Express (Illumina, Inc, San Diego, CA, USA).

The male samples and female samples were analyzed separately. To reduce the number of tests, we focused on identifying *cis* mQTLs located within 500 kb from the start or end of the DMR (or position of the significant CpG) [47]. We additionally required SNPs to (1) have a minor allele frequency of at least 1%, (2) be imputed with good certainty: information metric (info score) ≥ 0.4 , and (3) be associated with AD case–control status (as determined by clinical consensus diagnosis of cognitive status), after adjusting for age, batch, and the first 3 PCs estimated from genotype data, at nominal P -value less than 0.05. Next, for the ROSMAP methylation residuals obtained in section “Integrative methylation—gene expression analysis”, we fit the linear model ROSMAP methylation residual \sim SNP dosage + batch + PC1 + PC2 + PC3, where PC1, PC2, and PC3 are the first three PCs estimated from genotype data, to test the association between methylation residuals in CpGs and the imputed allele dosages for SNPs to identify mQTLs. The analysis for DMRs was the same except that we replaced ROSMAP methylation residual with median (ROSMAP methylation residuals) of all CpGs located within the DMR. SNPs with FDR less than 0.05 in the linear model described above were considered to be significant mQTLs.

Drug target analysis

We compared our list of sex-specific DNA methylation differences with targets of drugs prescribed to AD patients or in the development for AD in the ChEMBL database [48] (<https://www.ebi.ac.uk/chembl/>). To this end, we overlapped genes mapped to significant CpGs or DMRs with the genes targeted by compounds annotated to “Alzheimer Disease” in ChEMBL.

Results

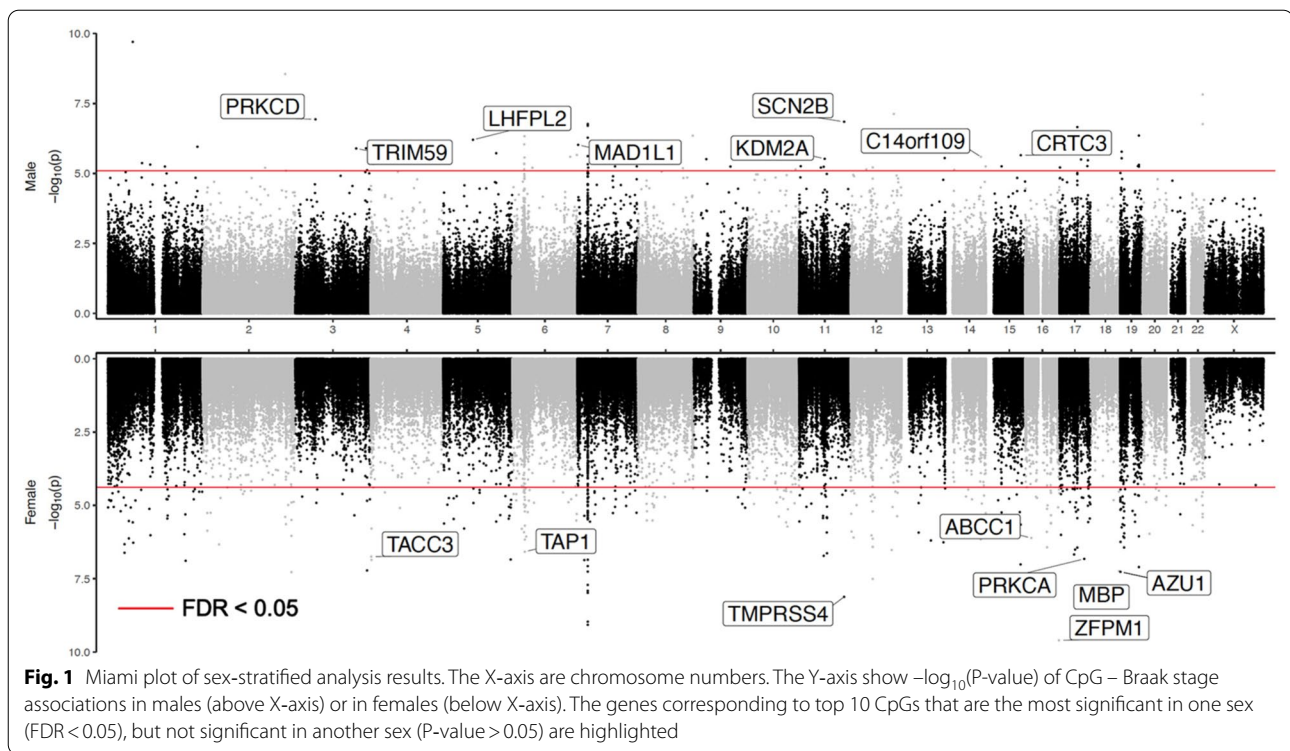
Description of EWAS cohorts and data

Among the four cohorts (Additional file 2: Table S1), the mean age at death ranged from 79.3 to 87.2 years in females and from 67.5 to 85.0 years in males. The number of CpGs and samples removed at each quality control step are presented in Additional file 2: Table 2. For females, inflation factor lambdas (λ) by the conventional approach ranged from 1.060 to 1.154, and lambdas based on the *bacon* approach [32] (λ_{bacon}) ranged from 1.021 to 1.059 (Additional file 1: Fig. S1). Similarly, for males, λ ranged from 0.906 to 1.265, and λ_{bacon} ranged from 0.957 to 1.114. These values are comparable to those obtained in other recent large-scale EWAS [49].

Sex-specific DNA methylation differences in AD neuropathology

In the sex-stratified analysis, at 5% FDR, our meta-analysis identified 381 and 76 CpGs, mapped to 245 and 51 genes in female and male samples, respectively (Fig. 1, Table 1, Additional file 2: Tables S3, S4). Similarly, at 5% FDR, we also identified 72 and 27 DMRs, mapped to 66 and 22 genes, in female and male samples, respectively (Table 2, Additional file 2: Tables S5, S6). Among them, 3.6% (16 out of 441 unique FDR-significant CpGs) and 12.5% (11 out of 88 unique FDR-significant DMRs) were significant in both females and males with the same direction of change. The average number of CpGs per DMR was 6.5 ± 8.9 . Also, the FDR-significant methylation differences at CpGs and DMRs did not completely overlap. Only 89 out of the 381 (23.4%) significant CpGs in females, and 13 out of the 76 (17.1%) significant CpGs in males overlapped with the significant DMRs. Among all CpGs and all DMRs, the effect estimates in males and females correlated only modestly ($r_{CpG} = 0.124$, $r_{DMR} = 0.170$, Additional file 1: Fig. S2), and about half (53% of CpGs, 54% of DMRs) were in the same direction of change in males and females, similar to what would be expected by chance.

In sex-by-Braak stage interaction analysis, we identified significant interaction at 14 CpGs, but no significant interactions at DMRs at 5% FDR. There was also little overlap between significant DNA methylation differences identified in sex-stratified and sex-by-Braak stage interaction analyses. Only 4 CpGs were identified by both analyses (Table 3). To understand this discrepancy, note that the sex-stratified analysis detected many differences that are attenuated but might be in the same direction in one sex group compared to the other. More specifically, among the FDR-significant CpGs identified in the sex-stratified analysis, many of them (370 out of 381 significant CpGs in the analysis of female samples, and 65 out of 76 significant CpGs in the analysis



of male samples) had the same direction of change for methylation-Braak stage association in both sexes (Additional file 2: Tables S3, S4). In Table 1, among the 10 most significant CpGs from the sex-stratified analysis, 9 female-specific and 6 male-specific CpGs had the same direction of methylation-Braak stage association in both sexes. On the other hand, in sex-by-Braak stage interaction analysis, 13 out of the 14 significant CpGs had the opposite directions of differences for methylation-Braak stage associations in females and males (Table 3). Therefore, the interaction analysis was able to identify CpGs with large differences in sex-specific effect estimates, often in different directions, but these effects might not have reached FDR significance in sex-stratified analysis. For example, in Table 3, the CpG with the most significant interaction (cg13212831) had effect estimates of 0.083 and -0.139 for females and males, respectively. In sex-stratified analysis, although the methylation-Braak stage associations were highly significant ($P\text{-value}_{\text{female}} = 0.006$, $P\text{-value}_{\text{male}} = 4.1 \times 10^{-5}$), they did not reach 5% FDR significance threshold ($FDR_{\text{female}} = 0.413$, $FDR_{\text{male}} = 0.097$). Therefore, the results from sex-stratified analysis and sex-by-Braak stage interaction analysis complemented each other.

Enrichment analysis of sex-specific DNA methylation differences across genomic features

Figure 2 presents an overview of the enrichment analysis results. Compared to background probes, significant hypermethylated DMRs and CpGs in females are over-represented in CpG islands and gene bodies (Additional file 1: Fig. S3a, Additional file 2: Table S7). Significant hypermethylated DMRs and CpGs in males are over-represented in CpG island shores, 5'UTRs, and TSS1500s. In contrast, significant hypomethylated differences in females and males are over-represented in open seas (Additional file 1: Fig. S3b, Additional file 2: Table S7). These observations are consistent with the knowledge that during aging, human brain DNA methylation levels gradually increase (hypermethylation) at genomic loci located at CpG islands and gene promoters, whereas intergenic CpG sites are marked with hypomethylation [50, 51].

Our enrichment analysis for chromatin states showed that significant hyper-methylated differences in females were enriched in bivalent enhancer, flanking active TSS, repressed polycomb, and transcription at gene 5' and 3' regions (Additional file 1: Fig. S3c, Additional file 2: Table S8). On the other hand, significant hypermethylated differences in males were enriched in active TSS, flanking active TSS, and repressed polycomb regions. Hypomethylated differences in females were enriched in enhancers, weak repressed polycomb, and weak

Table 1 Top 10 CpGs in sex-stratified analysis. Shown are CpGs that are highly significant in one sex (FDR < 0.05), but not significant (P-value > 0.05) in the other sex. For each CpG, annotations include the location of the CpG based on hg19/GRCh37 genomic annotation (Chr, position), Illumina gene annotations, nearby genes based on GREAT, and chromatin state. The inverse-variance weighted meta-analysis regression model results include estimated effect size (estimate) where CpGs that are hyper-methylated in samples with AD neuropathology have positive values, and its associated standard error (se), P-value, and false discovery rate (FDR) for multiple comparison corrections. Bold indicates a significant association at 5% FDR

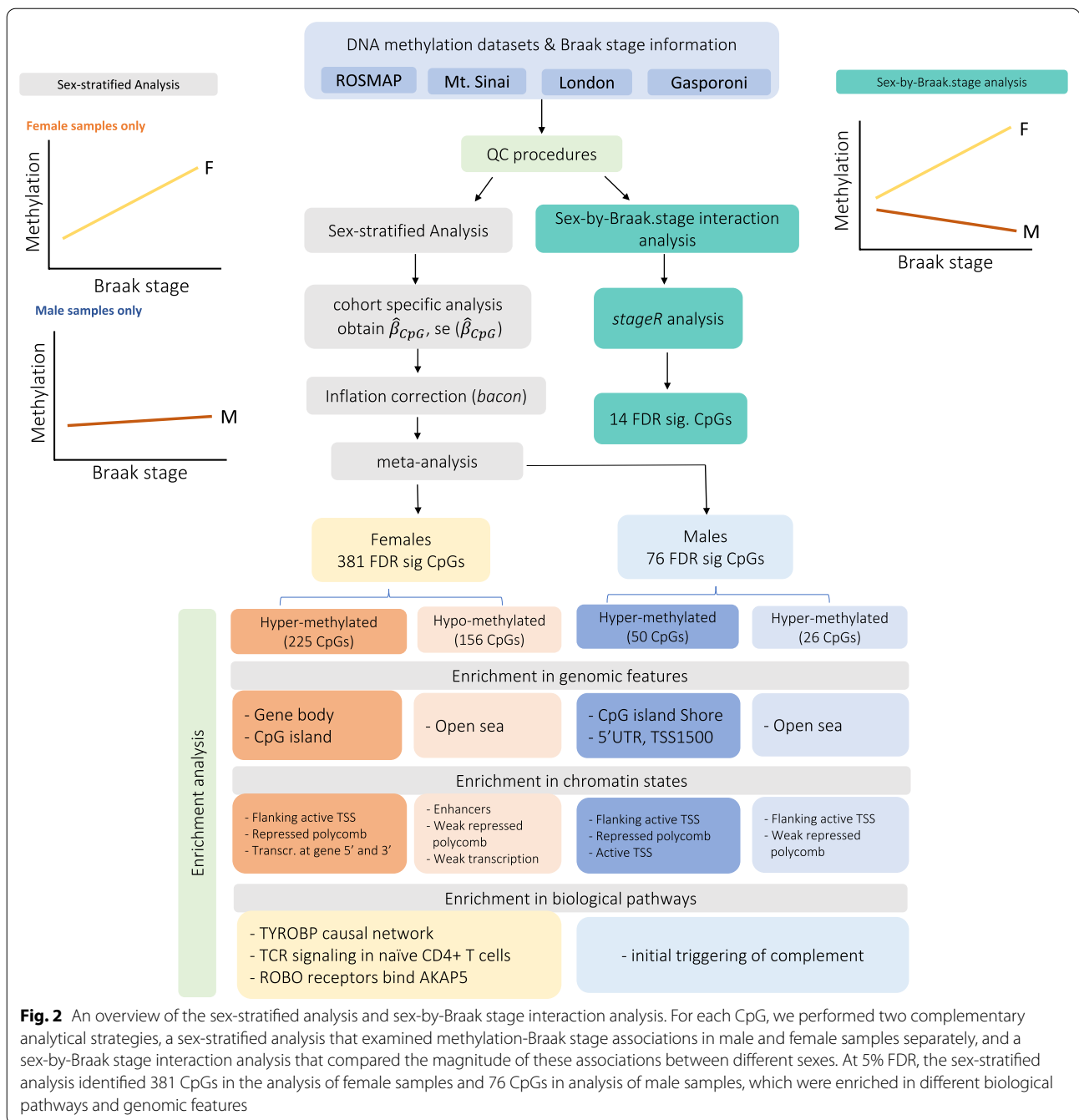
cpg	Annotations			Female samples				Males samples				
	chr	Position	Illumina	GREAT (distance to TSS)	chromatin state	estimate se	P-value	FDR	estimate se	P-value	FDR	
<i>Significant only in female samples</i>												
cg09502865	chr16	88600155	ZFPM1	ZC3H18(-36633); ZFPM1(+80431)	Active TSS	0.179	0.028	2.50E-10	0.094	0.034	4.46E-01	9.64E-01
cg05235171	chr11	117958104	TMPRSS4	TMPRSS4(+10301); SCN4B(+65430)	Quiescent/Low	-0.168	0.029	7.61E-09	-0.025	0.033	4.47E-01	9.64E-01
cg15610437	chr19	827821	AZU1	AZU1(-4)	Weak Repressed PolyComb	-0.155	0.029	5.45E-08	-0.090	0.034	9.79E-02	8.25E-01
cg13572782	chr18	74799495	MBP	MBP(+45229); ZNF236(+263380)	Active TSS	0.157	0.029	5.75E-08	0.047	0.036	1.90E-01	8.92E-01
cg17881200	chr7	27138850		HOXA1(-3258)	Repressed PolyComb	0.152	0.029	1.41E-07	0.131	0.034	6.22E-02	7.73E-01
cg22632947	chr17	64787784	PRKCA	CACNG5(-43450); PRKCA(+488841)	Flanking Active TSS	-0.139	0.026	1.50E-07	-0.005	0.028	8.57E-01	9.95E-01
cg15467503	chr4	1727234	TACC3	TMEM129(-4177); TACC3(+3969)	Weak transcription	-0.146	0.028	1.81E-07	-0.083	0.034	1.33E-01	8.59E-01
cg26033526	chr6	32819858	TAP1	PSMB9(-2079); TAP1(+1896)	Genic enhancers	0.148	0.029	2.64E-07	-0.021	0.034	5.23E-01	9.73E-01
cg08363067	chr16	16170085	ABCC1	ABCC1(+126652); ABCC6(+147235)	Weak transcription	-0.120	0.024	7.68E-07	-0.050	0.028	7.41E-02	7.94E-01
cg12926693	chr6	36665611		RAB44(-17644); CDKN1A(+19125)	Quiescent/Low	-0.149	0.030	8.59E-07	-0.067	0.035	5.19E-02	7.52E-01
<i>Significant only in male samples</i>												
cg07687398	chr3	53198666	PRKCD	PRKCD(+3531); TKT(+91371)	Weak transcription	0.052	0.030	8.63E-02	0.183	0.035	1.16E-07	9.88E-03
cg10513118	chr11	118047203	SCN2B	SCN2B(+184)	Active TSS	0.038	0.030	2.01E-01	0.172	0.033	1.42E-07	9.88E-03
cg21253952	chr8	143662999		ARC(+33833); BAI1(+132209)	Weak Repressed PolyComb	-0.019	0.030	5.33E-01	0.169	0.034	4.44E-07	1.53E-02
cg18281939	chr5	77783895	LHFPL2	SCAMP1(+127557); LHFPL2(+160752)	Weak transcription	-0.022	0.029	4.55E-01	-0.179	0.036	6.26E-07	1.79E-02
cg11809272	chr6	31409361		HLA-B(-84398); MICB(-56530)	Quiescent/Low	-0.001	0.031	9.77E-01	0.161	0.033	9.08E-07	2.17E-02
cg15952933	chr7	1899886	MAD1L1	ELFN1(+172132); MAD1L1(+372991)	Weak transcription	-0.058	0.033	7.56E-02	-0.156	0.032	9.48E-07	2.17E-02
cg11614451	chr3	160167729	TRIM59	ENS00000248710(-113); TRIM59(-113)	Flanking Bivalent TSS/Enh	-0.041	0.029	1.56E-01	-0.150	0.031	1.28E-06	2.44E-02
cg18942110	chr15	91072797	CRTC3	CRTC3(-502)	Active TSS	0.031	0.030	3.06E-01	-0.164	0.035	2.23E-06	3.19E-02
cg01655008	chr14	93652954	C14orf109	MOAPI(-1687); TMEM251(+1597)	Transcr. at gene 5' and 3'	-0.042	0.029	1.51E-01	-0.152	0.032	2.54E-06	3.33E-02
cg02331272	chr11	66964208	KDM2A	ADRBK1(-69672); KDM2A(+77051)	Weak transcription	0.058	0.030	1.10E-01	-0.166	0.036	2.99E-06	3.52E-02

Table 2 Top 10 and 6 DMRs in sex-stratified analysis. Shown are DMRs that are highly significant in one sex (FDR<0.05), but not significant (P-value>0.05) in another sex. Only 6 DMRs satisfied these criteria in male samples. For each DMR, annotations include the location of the DMR based on hg19/GRCh37 genomic annotation (DMR), Illumina gene annotations, nearby genes based on GREAT, and chromatin state. The inverse-variance weighted meta-analysis regression models results based on coMethDMR include estimated effect size (estimate) where DMRs that are hyper-methylated in samples with AD neuropathology have positive values; its associated standard error (se), P-value, and false discovery rate (FDR) for multiple comparison corrections. Shown in bold are significant results with FDR<0.05

DMR	Annotations			Female samples			Male samples				
	Illumina	GREAT (distance to TSS)	chromatin state	estimate se	P-value	FDR	estimate se	P-value	FDR		
<i>Significant only in female samples</i>											
chr5:27038605-27038836	CDH9	CDH9(-28)	Active TSS;Flanking Active TSS	0.128	0.024	1.87E-07	2.30E-03	0.077	0.027	2.74E-01	8.99E-01
chr15:31621629-31621843	KLF13	KLF13(+2678); OTUD7A(+325806)	Active TSS	0.115	0.023	3.30E-07	2.30E-03	0.042	0.027	1.19E-01	8.07E-01
chr18:74799495-74799572	MBP	MBP(+45191); ZNF236(+263418)	Active TSS	0.138	0.028	5.81E-07	2.48E-03	0.049	0.033	1.30E-01	8.13E-01
chr7:45066738-45067057	CCM2	CCM2(+273)	Weak transcription	-0.125	0.026	2.23E-06	6.20E-03	-0.090	0.027	5.51E-02	7.00E-01
chr13:67803895-67804060	PCDH9	PCDH9(+490)	Active TSS	-0.088	0.019	5.04E-06	1.02E-02	-0.017	0.022	4.40E-01	9.50E-01
chr16:66969401-66969506	CES2;FAM96B	FAM96B(-1151); CES2(+1091)	Flanking Active TSS	0.115	0.025	5.68E-06	1.02E-02	0.052	0.028	6.52E-02	7.28E-01
chr15:40268421-40268777	EIF2AK4	EIF2AK4(+42245); SRP14(+62790)	Active TSS	0.125	0.028	7.12E-06	1.16E-02	-0.005	0.032	8.72E-01	9.94E-01
chr5:14492774-14492945	TRIO	FAM105B(-171997); TRIO(+349049)	Strong transcription	-0.103	0.023	8.25E-06	1.24E-02	-0.009	0.029	7.49E-01	9.85E-01
chr17:56736571-56737118	TEX14	SEPT4(-118666); TEX14(+32539)	Active TSS	-0.070	0.016	9.13E-06	1.26E-02	0.017	0.017	3.20E-01	9.16E-01
chr17:46651722-46651952	HOXB3	HOXB3(-20553); HOXB4(+5636)	Repressed PolyComb	0.113	0.025	9.24E-06	1.26E-02	0.030	0.027	2.63E-01	8.97E-01
<i>Significant only in male samples</i>											
chr17:1173700-1173767	BHLHA9	BHLHA9(-119)	Weak Repressed PolyComb	-0.041	0.025	1.07E-01	8.23E-01	-0.118	0.026	5.08E-06	1.59E-02
chr11:68780866-68780984	MIRGPRF	MIRGPRF(-48)	Flanking Bivalent TSS/Enh	0.032	0.024	1.80E-01	8.93E-01	0.112	0.026	1.16E-05	2.96E-02
chr12:52437299-52437571	PTPN21	C12orf44(-26320); NR4A1(+20819)	Enhancers	0.009	0.017	5.93E-01	9.93E-01	0.075	0.017	1.38E-05	3.31E-02
chr14:89017615-89017776	PTPN21	PTPN21(+3381); SPATA7(+165822)	Active TSS	0.046	0.024	6.03E-02	7.31E-01	0.102	0.024	1.46E-05	3.31E-02
chr19:17691465-17691691	GLT2SD1	COLGALTI(+25175); UNCI3A(+107430)	Strong transcription	-0.006	0.022	8.06E-01	1.00E+00	0.107	0.025	2.47E-05	4.16E-02
chr6:32920567-32921233	HLA-DMA	ENSG00000248993(-1); HLA-DMA(-1)	Flanking Active TSS; Active TSS; Quiescent/Low	-0.045	0.024	3.16E-01	9.56E-01	-0.117	0.028	3.17E-05	4.78E-02

Table 3 Results from sex-by-Braak stage interaction analysis. For each CpG, annotations include the location of the CpG based on hg19/GRCh37 genomic annotation (chr, position), Illumina gene annotations, nearby genes based on GREAT, and chromatin state. The inverse-variance weighted meta-analysis regression model results include estimated effect size (estimate) where CpGs that are hyper-methylated in samples with AD neuropathology have positive values, its associated standard error (se), and P-value. Adj.pval is adjusted P-value from stageR analysis. Shown in bold are significant results (adj.pval < 0.05 for interaction and P-value < 0.05 for one sex). * indicates these CpGs also reached 5% FDR significance in sex-stratified analysis

cpg	Annotations			Female samples			Male samples			Sex * Braak stage interaction					
	chr	Position	Illumina	GREAT (distance to TSS)	chromatin state	estimate	se	P-value	estimate	se	P-value	estimate	se	P-value	adj.pval
cg13212831	chr1	56046343		USP24(-365558); PPAP2B(+998897)	Weak transcription	0.083	0.030	6.15E-03	-0.139	0.034	4.10E-05	-0.222	0.044	6.38E-07	3.54E-04
cg25734825	chr3	119182523	TMEM39A	TMEM39A(+5)	Active TSS	0.059	0.030	5.01E-02	-0.156	0.036	1.21E-05	-0.220	0.045	1.12E-06	6.22E-04
*cg02331272	chr11	66964208	KDM2A;KDM2A	ADRBK1(-69672); KDM2A(+77051)	Weak transcription	0.058	0.030	1.10E-01	-0.166	0.036	2.99E-06	-0.215	0.046	2.25E-06	1.25E-03
cg10622825	chr1	172413349	PIGC;PIGC;Tor105	PIGC(-124)	Active TSS	-0.069	0.030	2.22E-02	0.134	0.034	7.78E-05	0.200	0.045	7.00E-06	3.88E-03
cg10784067	chr16	14014435	ERCC4	ERCC4(+422)	Active TSS	-0.127	0.032	5.33E-05	0.068	0.033	3.78E-02	0.201	0.045	9.03E-06	5.01E-03
cg14284055	chr1	24439399	MYOM3	MYOM3(-735)	Bivalent Enhancer	0.115	0.029	8.28E-05	-0.066	0.037	7.12E-02	-0.193	0.045	1.94E-05	1.07E-02
*cg18942110	chr15	91072797	CRTC3;CRTC3	CRTC3(-502)	Active TSS	0.031	0.030	3.06E-01	-0.164	0.035	2.23E-06	-0.187	0.045	3.13E-05	1.74E-02
cg09342330	chr14	89021109	PTPN21;PTPN21	PTPN21(-33)	Active TSS	0.045	0.030	1.31E-01	-0.144	0.037	8.30E-05	-0.189	0.046	3.47E-05	1.93E-02
cg21722170	chr6	31977443	TXN8;TXN8	C4B(-5095); C4A(+27643)	Quiescent/Low	0.034	0.030	2.53E-01	-0.148	0.034	1.57E-05	-0.183	0.045	4.17E-05	2.31E-02
cg03662217	chr21	35747882	FAM165B	SMIM11(-20)	Active TSS	0.039	0.029	1.85E-01	-0.141	0.036	7.27E-05	-0.184	0.045	4.59E-05	2.55E-02
cg15026265	chr12	28283812		PTHUH(-158910); CCDC91(-59566)	Quiescent/Low	-0.038	0.029	1.95E-01	0.134	0.033	6.58E-05	0.176	0.044	6.72E-05	3.73E-02
cg00659421	chr7	86781760	DMTF1;DMTF1;DMTF1;DMTF1;DMTF1;DMTF1	DMTF1(-109)	Active TSS	-0.050	0.031	1.08E-01	0.130	0.033	7.53E-05	0.178	0.045	6.95E-05	3.86E-02
*cg24917065	chr8	23418389	SLC25A37	SLC25A37(+32072); NKX3-1(+122050)	Quiescent/Low	-0.135	0.030	6.26E-06	0.042	0.033	2.05E-01	0.174	0.044	6.98E-05	3.87E-02
*cg18281939	chr5	77783895	LHFPL2	SCAMP1(+127557); LHFPL2(+160752)	Weak transcription	-0.022	0.029	4.55E-01	-0.179	0.036	6.26E-07	-0.177	0.045	7.10E-05	3.94E-02



transcription regions, while hypomethylated differences in males were enriched in flanking active TSS and weak repressed polycomb regions (Additional file 1: Fig. S3d, Additional file 2: Table S8). Notably, the enrichment of hypermethylated differences in repressed polycomb regions in both female and male samples is consistent with our previous sex-combined meta-analysis, which also highlighted the enrichment of hyper-methylated Braak-associated DNA methylation differences in polycomb repressed regions [22].

Similarly, enrichment tests for regulatory elements using the LOLA software also supported the potential functional relevance of these significant differences in DNA methylation. Significant DMRs and CpGs in females and males were both enriched in binding sites of EZH2 and SUZ12 (Additional file 2: Table S9), which are subunits of polycomb repressive complex 2 (PRC2), consistent with the observed enrichment of methylation differences in PRC2 repressed regions (Additional file 1:

Fig. S3c) and previous observations that DNA methylation often interact with PRC2 binding [52, 53]. PRC2 is a type of polycomb group (PcG) protein and plays important roles in multiple biological processes including proliferation and differentiation as well as maintenance of cellular identity through regulation of gene expression. Of particular relevance to AD, PRC2 silences genes involved in neurodegeneration and its deficiency leads to the de-repression of developmental regulators such as the Hox gene clusters, which manifest in progressive and fatal neurodegeneration in mice [54].

Gene ontology and pathway analysis

Because of the relatively smaller number of gene sets being tested, a 25% FDR significance threshold, instead of the conventional 5% FDR, was suggested for GSEA [55]. At 25% FDR, the significant DNA methylation differences in females were enriched in TYROBP causal network (FDR=0.014), TCR signaling in naïve CD4+ T cells (FDR=0.130) and ROBO receptors bind AKAP5 (FDR=0.160) gene sets, and significant methylation differences in males were enriched in the initial triggering of complement gene set (FDR=0.245). The TYROBP causal network was previously inferred from a large-scale network analysis of human late-onset AD brains [56]; it was FDR significant (P-value < 0.001, FDR=0.014) in females (Additional file 1: Fig. S4a), compared to a nominal association in males (P-value < 0.001, FDR=0.620). Interestingly, the core enrichment subset of genes identified by GSEA in the female and male networks regulated by TYROBP involved DNA methylation differences at different genes (Additional file 1: Fig. S4b), highlighting different regulatory mechanisms for this gene network in males and females.

The comparison with gene ontology (GO) terms showed at 25% FDR, significant methylation differences in females were enriched in 25 GO biological processes (Table 4, Additional file 2: Table S10), many of which are involved in inflammatory responses associated with AD pathology including CD8 positive alpha beta T cell activation and interferon alpha production, as well as other biological processes critical for AD pathogenesis such as response to platelet derived growth factor and positive regulation of axon extension. For males, we did not identify any significant GO terms at 25% FDR; the strongest enrichment with nominal P-value less than 0.001 involved immune responses to the accumulation of amyloid- β (A β) in the brain, such as regulation of T cell activation via T cell receptor contact with antigen bound to MHC molecule on antigen presenting cell, and other biological processes recently implicated in AD such as response to angiotensin [57, 58] and cell redox homeostasis [59, 60].

Correlation of sex-specific DNA methylation differences in AD neuropathology with expression levels of nearby genes

At 5% FDR, among FDR significant CpGs in females, all 381 CpGs were linked to a nearby gene by GREAT software, in which 14 were significantly associated with target gene expression levels (Additional file 2: Table S11), and half of them (n=7) had effects in the negative direction. Among FDR significant CpGs in males, out of the 46 CpGs that were linked to a nearby gene, 2 were significantly associated with target gene expression and both were in the negative direction. Notably, in females, several of the most significant CpG methylation-gene expression associations were observed for the *HLA-DPA1* gene, which encodes microglia receptors involved in antigen presentation and is regulated by PU.1 [61]. In males, the most significant CpG-gene expression was for *HLA-DRB1*, another PU.1 target gene [61]. For the 14 CpGs identified by our sex-by-Braak stage interaction analysis, only one CpG (cg24917065) was significantly associated with target gene (*SLC25A37*) expressions.

Correlation and overlap of sex-specific DNA methylation differences in AD neuropathology with genetic susceptibility loci

To evaluate if the significant methylation differences are located in the vicinity of sex-specific genetic variants implicated in AD, we compared our sex-specific CpGs and DMRs with the recently identified sex-specific SNPs associated with AD biomarkers [62] or AD pathology [63]. We found only 5 CpGs, mapped to the *SERP2*, *KCNE1*, *TNKS1BP1*, *FAM165B*, *PLCB4* genes were located within 500 kb of the sex-specific SNPs (Additional file 2: Table S12).

To search for mQTLs, which are genetic variants associated with DNA methylations, we next tested associations between the sex-specific CpGs and DMRs with SNPs that are located within 500 kb from them using 434 female samples, 254 male samples from the ROSMAP study, which had both genotype and DNA methylation data. While no mQTL-DMR pairs reached 5% FDR significance, we did identify 572 and 284 FDR-significant mQTL-CpG pairs associated with the sex-specific CpGs in females and males, respectively (Additional file 2: Tables S13, S14). Among the 381 and 76 sex-specific CpGs identified in female and male samples, respectively, 41 (11%) and 15 (20%) had at least one corresponding mQTL in brain samples. Among the 14 CpGs identified in our sex-by-Braak stage interaction analysis, 2 and 7 CpGs with at least one brain mQTL, corresponding to 21 and 236 significant mQTL-CpG pairs, were identified at 5% FDR in females and males, respectively (Additional file 2: Table S15). These mQTL-CpG pairs point to

important potential molecular mechanisms of disease-associated genetic variants that might due, at least in part, to their influences on DNA methylations, which can be further validated in mechanistic studies.

Drug target analysis of sex-specific DNA methylation differences

To investigate the clinical impact of the sex-specific DNA methylation differences, we next compared them with targets of drugs in the ChEMBL database [48] that are annotated to Alzheimer's disease, many of which are antipsychotic medications commonly prescribed to AD patients for treating psychiatric symptoms that accompany AD. We found that 13 CpGs and 2 DMRs, mapped to 20 genes, had overlap with targets of 16 different drugs (Additional file 2: Table S16). Among them, *CACNA1C* encodes a voltage-dependent calcium channel, which is a target of cholinesterase inhibitor donepezil. Previously, drug responses for donepezil were shown to be modulated by the sex hormone estrogen receptor alpha (*ESR1*) genotype [64]. Several CpGs and one DMR are mapped to targets of valproic acid, a mood stabilizer often prescribed for AD patients and was shown to have different pharmacokinetic profiles between male and female subjects [65]. Interestingly, two CpGs and 1 DMR also mapped to targets of caffeine, which was included in cocktail therapy in AD clinical trials [66, 67]. Although caffeine reduces the risk for AD [68, 69] in both men and women, the protective effect seems to be greater in women [70]. Also, *CHRM3* encodes muscarinic acetylcholine receptor, which is targeted by two commonly prescribed antipsychotic drugs for AD patients, trazodone and haloperidol. In both human and animal models, it has been observed treatment with haloperidol induces sex-specific DNA methylation differences [71, 72]. While this study could not establish the mechanisms at which DNA methylation interacts with drugs that AD patients take, we hypothesize that these might include the influence of DNA methylation on drug responses or the differences in DNA methylation resulted from drug actions.

Discussion

To identify sex-specific differences in AD neuropathology, we performed a sex-stratified analysis and a sex-by-Braak stage interaction analysis for each cohort and then used a meta-analysis strategy to combine the cohort-specific association signals. In the sex-stratified analysis, as discussed above, a substantial number of the significant loci showed the same direction but attenuation of effect size for methylation-Braak stage association in a different sex (Tables 1, 2). Therefore, it is not surprising that many of these significant CpGs were identified previously in sex-combined meta-analysis [22]. Among FDR

significant methylation differences in females, 325 CpGs (85%) and 40 DMRs (56%), mapped to genes such as *HOXA3*, *AZU1*, and *MBP* were also previously identified in our sex-combined meta-analysis [22] (Additional file 2: Tables S3, S5). Similarly, in the analysis of male samples, among FDR significant differences, 58 (76%) CpGs and 15 DMRs (56%), mapped to genes such as *MAMSTR*, *RHBDF2*, and *AGAP2*, overlapped with significant hits from sex-combined meta-analysis [22] (Additional file 2: Tables S4 and S6). However, our sex-specific analysis provided the new insight that the effects of these known AD genes appear to be predominately driven by effects in only one sex (Tables 1, 2).

On the other hand, our sex-specific analysis also uncovered novel methylation differences at 84 CpGs and 42 DMRs that were not identified previously by sex-combined analyses [22], which may had reduced power due to heterogeneity between the sexes. For example, among the top 10 CpGs in the sex-stratified analysis (Table 1), a new locus at cg22632947, which mapped to the gene body of the *PRKCA* gene, was highly significant in female samples (estimate = -0.139 , P-value = 1.50×10^{-7} , FDR = 3.00×10^{-3}), but not significant in male samples (estimate = -0.005 , P-value = 0.857 , FDR = 0.995) (Additional file 1: Fig. S5). The *PRKCA* gene encodes protein kinase C α (PKC α), which participates in synaptic loss resulting from the accumulation of amyloid- β (A β) in AD neuropathology [73, 74]. Another novel locus is at cg18942110 in the promoter of the *CRTC3* gene, where methylation-Braak stage association was highly significant in male samples (estimate = -0.164 , P-value = 2.23×10^{-6} , FDR = 3.19×10^{-2}), but not significant in female samples (estimate = -0.031 , P-value = 0.306 , FDR = 0.952) (Additional file 1: Fig. S5). *CRTC3* is a member of the *CRTC* family, which are coactivators of the transcription factor CREB (cAMP-response element binding protein). In addition to its crucial role in maintaining synaptic plasticity and facilitation of short-term memory to long-term memory, the CREB signaling pathway also mediates synapse loss induced by A β in AD [75]. Notably, synapse loss significantly correlates with cognitive impairment [76, 77] and has been observed to be an early feature of AD pathogenesis [78, 79].

The sex-by-Braak stage interaction analysis also uncovered several additional novel methylation loci that affected AD neuropathology in a sex-specific manner. Notably, none of the 14 CpGs detected in our interaction analysis was identified in previous large-scale DNA methylation studies [18–22], suggesting that sex-specific differences such as these can be missed by conventional studies that do not consider the impact of sex. This is likely due to the cancelation of effects in sex-combined

analysis because the majority of these 14 CpGs had different directions of methylation-Braak stage effects in male and female samples (Table 3). Among genes mapped to these 14 CpGs, *TMEM39A* is a member of the transmembrane (TMEM) protein family. In recent GWAS, a genetic variant on *TMEM39A* was discovered and replicated as an important risk locus for multiple sclerosis, an autoimmune condition of the central nervous system [80, 81]. While relatively little is known about the role of *TMEM39A* in AD, given its important contributions to inflammation, dysregulated type I interferon responses, and other immune processes [82] which are also implicated in AD, methylation differences affecting this gene are particularly relevant. Another noteworthy gene is *TNXB* and its pseudogene *TNXA*, which are located in the major histocompatibility complex (MHC) class III region on chromosome 6. *TNXB* encodes tenascin proteins, which are extracellular matrix glycoproteins demonstrated to modulate synaptic plasticity in the brain [83]. In particular, genetic variants at the *HLA-DQB1* locus discovered in the recent AD genetic meta-analysis [84] included eQTLs for *TNXB/TNXA* in brain tissues [84, 85].

Consistent with previous studies [18, 19, 86, 87], we observed the majority of these sex-specific differences were hyper-methylated in samples with AD neuropathology, for which methylation levels increased as the AD Braak stage increased (Additional file 2: Tables S17, S18). More specifically, 59% of the significant CpGs and 69% of the significant DMRs in females, along with 66% of the significant CpGs and 89% of the significant DMRs in males were hyper-methylated in samples with AD neuropathology (Additional file 2: Tables S3–S6).

To better understand the relevance of these Braak-associated sex-specific differences, we also compared our results with several previous studies. The comparison with Xia et al. [16] and Xu et al. [17], which examined differential methylation between males and females in the prefrontal cortex, but without considering AD neuropathology [16, 17], showed our results were largely distinct. Among 451 unique CpGs identified in our sex-stratified analysis or sex-by-Braak stage interaction analysis, only 16 were also identified in Xia et al. [16] and none were identified in Xu et al. [17] (Additional file 2: Tables S3–S6). This is probably due to different hypotheses tested in our study and the sexual dimorphism studies – while our study examined the impact of sex on methylation-Braak stage association, the previous studies examined differential methylation between the sexes, regardless of AD neuropathology. The comparison of our results with sex-specific DNA methylation differences in fetal brain development [88, 89] also showed very little overlap (Additional file 2: Table S19); one hypothesis could be

that the Braak-associated sex-specific DNA methylation differences identified in this study might be influenced by environmental risk factors for AD, such as diet and exercise.

The results of our gene set analysis highlighted a number of critical sex-specific biological processes in AD neuropathology. Notably, the TYROBP causal network reached the FDR significance threshold in females (FDR=0.014) but was only nominally significant in males. Interestingly, Braak-associated CpG methylation differences that drove pathway associations (core enrichment genes) occurred at different genes in females and males (Additional file 1: Fig. S4), indicating a potentially sex-specific regulatory mechanism for this network. TYROBP (TYRO protein tyrosine kinase-binding protein) is a key regulator of the complement pathway in the immune/microglia network, which is activated as A β accumulates in LOAD brains [56, 90]. TYROBP is a transmembrane adaptor protein for TREM2, SIRP β 1, and CR3 receptors, which are known to be involved in AD pathogenesis [90–92]. Also, TYROBP is regulated by *SPI1*, a central hub for the network of genes involved in myeloid immune response in neurodegeneration [93]. In patients with LOAD, TYROBP was observed to be up-regulated in the brains in multiple cohorts [56]. Recent studies suggested TYROBP-mediated signaling is involved in multiple important functions as aggregating A β activates microglia, including enhanced phagocytosis of damaged neurons [56, 90] and suppression of inflammatory responses [94], as well as neuronal pruning activity [56]. Interestingly, in gene ontology (GO) analysis, among the most significant GO Biological Process terms (P-value<0.001) in females and males, none of them overlapped (Additional file 2: Table S10), even though the relevancy of all the top biological processes were supported by recent AD literature (Table 4). These results suggest different biological processes are associated with AD pathology in males and females.

Importantly, a number of these sex-specific biological processes pointed to important potential biomarkers and therapeutic targets for the treatment of AD. For example, one of the top biological processes enriched with significant methylation differences in female samples is response to platelet derived growth factor. Recently, multiple studies have shown that reduced levels of platelet-derived growth factors (PDGFs) in plasma significantly correlate with mild cognitive impairment and have proposed PDGFs as a potential biomarker for AD [95, 96]. For the significant methylation differences in male samples, one of the top biological processes highlighted by our enrichment analysis is dysregulation in the complement system. Recently, a number of novel agents targeting the complement system are being developed and

Table 4 Top 10 most significant GO Biological processes enriched with sex-specific DNA methylation differences associated with AD Braak stage in females and males. Shown are GSEA results including the number of genes in the gene set (SIZE), normalized enrichment score (NES), P-value, FDR, and relevant AD literature for the gene set

Gene Set	SIZE	NES	P-value	FDR	Relevance to AD
<i>Top 10 GO Biological Process terms in females</i>					
INTEGRIN_ACTIVATION	24	2.105	0	9.53E−02	Wennstrome et al. [98]
RESPONSE_TO_PLATELET_DERIVED_GROWTH_FACTOR	19	2.116	0	1.07E−01	Sil et al. [99]
I_KAPPAB_PHOSPHORYLATION	19	2.081	0	1.13E−01	Jha et al. [100]
NEGATIVE_REGULATION_OF_INTERLEUKIN_8_PRODUCTION	18	2.133	0	1.21E−01	Qin et al. [101]
POSITIVE_REGULATION_OF_MACROPHAGE_MIGRATION	25	2.048	0	1.46E−01	Bacher et al. [102]
TOLL_LIKE_RECEPTOR_SIGNALING_PATHWAY	142	2.031	0	1.61E−01	Fiebich et al. [103]
NEGATIVE_REGULATION_OF_TUMOR_NECROSIS_FACTOR_SUPERFAMILY_CYTOKINE_PRODUCTION	57	2.007	0	1.90E−01	Chang et al. [104]
REGULATION_OF_SYNCYTIUM_FORMATION_BY_PLASMA_MEMBRANE_FUSION	28	1.944	0	1.98E−01	Armoto et al. [105]
RESPONSE_TO_VITAMIN_A	19	1.945	0	2.08E−01	Ono et al. [106]
POSITIVE_REGULATION_OF_AXON_EXTENSION	42	1.931	0	2.08E−01	Kanaan et al. [107]
<i>Top 10 Biological Process terms in males</i>					
REGULATION_OF_T_CELL_ACTIVATION_VIA_T_CELL_RECEPTOR_CONTACT_WITH_ANTI-GEN_BOUND_TO_MHC_MOLECULE_ON_ANTIGEN_PRESENTING_CELL	6	1.869	0	5.98E−01	Schetters et al. [108]
REGULATION_OF_SYSTEMIC_ARTERIAL_BLOOD_PRESSURE_BY_CIRCULATORY_RENIN_ANGIOTENSIN	18	1.964	0	6.11E−01	Cosarderelioglu et al. [57]
NEGATIVE_REGULATION_OF_REACTIVE_OXYGEN_SPECIES_BIOSYNTHETIC_PROCESS	29	1.745	0	6.12E−01	Manoharan et al. [59]
COMPLEMENT_ACTIVATION	68	1.741	0	6.26E−01	Morgan [97]
RESPONSE_TO_ANGIOTENSIN	26	1.746	0	6.36E−01	Benigni et al. [58]
CELL_REDOX_HOMEOSTASIS	55	1.721	0	6.49E−01	Chen et al. [60]
PROTEIN_DEMETHYLATION	28	1.832	0	6.77E−01	Esposito et al. [109]
IMMUNE_RESPONSE_INHIBITING_CELL_SURFACE_RECEPTOR_SIGNALING_PATHWAY	6	1.781	0	7.02E−01	Schetters et al. [108]
DICARBOXYLIC_ACID_CATABOLIC_PROCESS	17	2.052	0	7.57E−01	Griffin et al. [110]
GLUTAMINE_FAMILY_AMINO_ACID_METABOLIC_PROCESS	70	1.657	0	7.75E−01	Conway et al. [111]

tested in clinical trials for potential effective therapy for AD [97]. Therefore, clinical trials testing potential treatment for AD patients might have more power for detecting treatment effects by considering sex and targeting the subgroup with the higher predicted benefit based on patient molecular profiles such as DNA methylation.

There are several limitations for this study. The methylation levels in the studies analyzed here were measured on the bulk prefrontal cortex, which contains a complex mixture of cell types. To reduce confounding effects due to cellular heterogeneities, we included the estimated neuron proportion of each brain sample as a covariate variable in all our analyses. Currently, a challenge with cell-type-specific studies is that they are often limited to smaller sample sizes due to labor-intensive sample preparation procedures and therefore have limited statistical power. Also, we did not identify any CpGs or DMRs from chromosome X, this might suggest that sex differences in AD neuropathology are not primarily due to chromosome X. Alternatively, the lack of association might also be due to the limited coverage by the 450k array. Future studies utilizing high throughput sequencing

that provides better coverage of the epigenome will help clarify the role of the X chromosome in AD neuropathology. Finally, the associations we identified in this study do not necessarily reflect causal relationships. Future studies that employ longitudinal designs are needed to identify causal changes in DNA methylation as AD initiates and progresses.

In summary, our study highlighted the importance of stratifying on sex and analyzing sex-by-disease interaction in the analysis of DNA methylation data to discover the epigenetic architectures underlying AD neuropathology. Our meta-analysis discovered many novel sex-specific DNA methylation differences consistently associated with the AD Braak stage in multiple studies. Because of cancelation of effects in different directions, or dilution from samples with no effect, these sex-specific effects would be missed by sex-combined analysis. Moreover, for many genes previously linked to AD neuropathology, our work provided evidence that the DNA methylation differences at these genes were predominately driven by effects in only one sex.

Our enrichment analysis highlighted divergent biological processes in males and females, which underscored sex-specific regulatory mechanisms involved in AD neuropathology. Finally, our results also have important implications for precision medicine—many of the sex-specific DNA methylation differences also pointed to important potential AD biomarkers and therapeutic targets, suggesting a pressing need for developing and applying sex-specific treatment strategies for AD.

Supplementary Information

The online version contains supplementary material available at <https://doi.org/10.1186/s40478-021-01177-8>.

Additional file 1: Supplementary Figures. **Figure S1.** Quantile-quantile (QQ) plots of observed and expected distributions of P-values in Gasparoni, London, Mount Sinai, and ROSMAP cohorts. **Figure S2.** Comparison of methylation-Braak stage associations in female samples and male samples. **Figure S3.** Enrichment of FDR-significant CpGs and CpGs located within FDR-significant DMRs with positive and negative effect estimates in various genomic features and chromatin states. **Figure S4.** Gene Set Enrichment of the TYROBP causal network with sex-specific Braak-associated DNA methylation differences. **Figure S5.** Forest plots for several top CpGs identified in sex-stratified analysis and sex-by-Braak stage interaction analysis.

Additional file 2: Supplementary Tables. **Table S1.** Sample information of the brain samples datasets included in the meta-analysis. **Table S2.** Quality control (QC) information on DNA methylation samples and probes for each cohort contributing to this meta-analysis. **Table S3.** In females, a total of 381 differentially methylated CpGs were significantly associated with the AD Braak stage at 5% FDR in the meta-analysis of four brain samples cohorts (Gasparoni, London, Mt. Sinai, ROSMAP). **Table S4.** In males, a total of 76 differentially methylated CpGs were significantly associated with the AD Braak stage at 5% FDR in the meta-analysis of four brain samples cohorts (Gasparoni, London, Mt. Sinai, ROSMAP). **Table S5.** In females, at 5% FDR, a total of 72 co-methylated DMRs were significantly associated with AD Braak stage in the meta-analysis of the four brain samples cohorts. **Table S6.** In males, at 5% FDR, a total of 27 co-methylated DMRs were significantly associated with AD Braak stage in the meta-analysis of four brain samples cohorts. **Table S7.** Enrichment of sex-specific DNA methylation changes in different genomic features. **Table S8.** Enrichment of sex-specific DNA methylation changes in different chromatin states. **Table S9.** Enrichment of sex-specific DNA methylation changes in binding sites of transcription factors and chromatin proteins assayed by ENCODE and CODEX projects. **Table S10.** Results of Gene Set Enrichment analysis of sex-specific CpGs and DMRs in female and males. **Table S11.** Significant association between sex-specific differences and expression levels of nearby genes. **Table S12.** The sex-specific CpGs and DMRs located within 500 kb of sex-specific SNPs associated with AD biomarkers or AD neuropathology. **Table S13.** mQTLs associated with FDR-significant CpGs in females. **Table S14.** mQTLs associated with FDR-significant CpGs in males. **Table S15.** mQTLs associated with significant CpGs identified by sex-by-Braak stage interaction analysis. **Table S16.** Sex-specific DNA methylation differences overlapped with AD drug targets in ChEMBL database. **Table S17.** Average beta values at each Braak stage for significant CpGs identified in female samples. **Table S18.** Average beta values at each Braak stage for significant CpGs identified in male samples. **Table S19.** Overlap of Braak-associated sex-specific CpGs and DMRs with sex-specific DNA methylation changes in fetal development.

Authors' contributions

L.W., J.Y., E.R.M., L.Z., T.C.S., L.G. designed the computational analysis. L.Z., T.C.S., L.G., M.S., J.C., L.W. analyzed the data. L.W., J.Y., E.R.M., X.C. contributed to the

interpretation of the results. L.Z., L.W. wrote the paper, and all authors read and approved the manuscript. L.W. conceived the original idea and supervised the project.

Funding

This research was supported by US National Institutes of Health grants R21AG060459 (L.W.), R01AG061127 (L.W.), R01AG062634 (E.R.M., L.W.), and R01AG060472 (E.R.M.). The ROSMAP study data were provided by the Rush Alzheimer's Disease Center, Rush University Medical Center, Chicago. Data collection was supported through funding by NIA grants P30AG10161, R01AG15819, R01AG17917, R01AG30146, R01AG36836, U01AG32984, U01AG46152, the Illinois Department of Public Health, and the Translational Genomics Research Institute.

Availability of data and materials

All datasets analyzed in this study are publicly available as described in Additional file 2: Table S1. The Mt. Sinai, London, Gasparoni, and ROSMAP datasets can be accessed from GEO (accessions [GSE80970](https://doi.org/10.1186/s40478-021-01177-8), [GSE59685](https://doi.org/10.1186/s40478-021-01177-8), [GSE66351](https://doi.org/10.1186/s40478-021-01177-8)) and Synapse (<https://doi.org/10.7303/syn3157275>). The scripts for the analysis performed in this study can be accessed at <https://github.com/TransBioloLab/ad-meta-analysis-by-sex>.

Declarations

Ethics approval and consent to participate.

Approval for ROSMAP dataset was obtained through Synapse. The ROSMAP study data were provided by the Rush Alzheimer's Disease Center, Rush University Medical Center, Chicago. Data collection was supported through funding by NIA grants P30AG10161, R01AG15819, R01AG17917, R01AG30146, R01AG36836, U01AG32984, U01AG46152, the Illinois Department of Public Health, and the Translational Genomics Research Institute.

Consent for publication

Not applicable.

Competing interests

The authors declare that they have no competing interests.

Author details

¹Division of Biostatistics, Department of Public Health Sciences, University of Miami, Miller School of Medicine, Miami, FL 33136, USA. ²Dr. John T Macdonald Foundation Department of Human Genetics, University of Miami, Miller School of Medicine, Miami, FL 33136, USA. ³John P. Hussman Institute for Human Genomics, University of Miami, Miller School of Medicine, Miami, FL 33136, USA. ⁴Brentwood High School, 5304 Murray Ln, Brentwood, TN 37027, USA. ⁵Sylvester Comprehensive Cancer Center, University of Miami, Miller School of Medicine, Miami, FL 33136, USA.

Received: 9 February 2021 Accepted: 10 April 2021

Published online: 26 April 2021

References

- Hurd MD, Martorell P, Delavande A, Mullen KJ, Langa KM (2013) Monetary costs of dementia in the United States. *N Engl J Med* 368(14):1326–1334
- Hebert LE, Weuve J, Scherr PA, Evans DA (2013) Alzheimer disease in the United States (2010–2050) estimated using the 2010 census. *Neurology* 80(19):1778–1783
- Koran MEI, Wagener M, Hohman TJ, I. Alzheimer's Neuroimaging (2017) Sex differences in the association between AD biomarkers and cognitive decline. *Brain Imaging Behav* 11(1):205–213
- Tschanz JT, Corcoran CD, Schwartz S, Treiber K, Green RC, Norton MC, Mielke MM, Piercy K, Steinberg M, Rabins PV, Leoutsakos JM, Welsh-Bohmer KA, Breitner JC, Lyketsos CG (2011) Progression of cognitive, functional, and neuropsychiatric symptom domains in a population cohort with Alzheimer dementia: the Cache County Dementia Progression study. *Am J Geriatr Psychiatry* 19(6):532–542

5. Ardekani BA, Convit A, Bachman AH (2016) Analysis of the MIRIAD data shows sex differences in hippocampal atrophy progression. *J Alzheimers Dis* 50(3):847–857
6. Holland D, Desikan RS, Dale AM, McEvoy LK, I. Alzheimer's Disease Neuroimaging (2013) Higher rates of decline for women and apolipoprotein E epsilon4 carriers. *AJNR Am J Neuroradiol* 34(12):2287–2293
7. Lin KA, Choudhury KR, Rathakrishnan BG, Marks DM, Petrella JR, Doraiswamy PM, I. Alzheimer's Disease Neuroimaging (2015) Marked gender differences in progression of mild cognitive impairment over 8 years. *Alzheimers Dement (N Y)* 1(2):103–110
8. Hua X, Hibar DP, Lee S, Toga AW, Jack CR Jr, Weiner MW, Thompson PM (2010) Sex and age differences in atrophic rates: an ADNI study with n=1368 MRI scans. *Neurobiol Aging* 31(8):1463–1480
9. Davis EJ, Broestl L, Abdulai-Saiku S, Worden K, Bonham LW, Minones-Moyano E, Moreno AJ, Wang D, Chang K, Williams G, Garay BI, Lobach I, Devidze N, Kim D, Anderson-Bergman C, Yu GQ, White CC, Harris JA, Miller BL, Bennett DA, Arnold AP, De Jager PL, Palop JJ, Panning B, Yokoyama JS, Mucke L, Dubal DB (2020) A second X chromosome contributes to resilience in a mouse model of Alzheimer's disease. *Sci Transl Med* 12:558
10. Lapane KL, Gambassi G, Landi F, Sgadari A, Mor V, Bernabei R (2001) Gender differences in predictors of mortality in nursing home residents with AD. *Neurology* 56(5):650–654
11. Stern Y, Tang MX, Albert MS, Brandt J, Jacobs DM, Bell K, Marder K, Sano M, Devanand D, Albert SM, Bylsma F, Tsai WY (1997) Predicting time to nursing home care and death in individuals with Alzheimer disease. *JAMA* 277(10):806–812
12. Dunn GA, Morgan CP, Bale TL (2011) Sex-specificity in transgenerational epigenetic programming. *Horm Behav* 59(3):290–295
13. Menger Y, Bettscheider M, Murgatroyd C, Spengler D (2010) Sex differences in brain epigenetics. *Epigenomics* 2(6):807–821
14. McCarthy MM, Nugent BM (2015) At the frontier of epigenetics of brain sex differences. *Front Behav Neurosci* 9:221
15. Burghardt KJ, Pilsner JR, Bly MJ, Ellingrod VL (2012) DNA methylation in schizophrenia subjects: gender and MTHFR 677C/T genotype differences. *Epigenomics* 4(3):261–268
16. Xia Y, Dai R, Wang K, Jiao C, Zhang C, Xu Y, Li H, Jing X, Chen Y, Jiang Y, Kopp RF, Giase G, Chen C, Liu C (2019) Sex-differential DNA methylation and associated regulation networks in human brain implicated in the sex-biased risks of psychiatric disorders. *Mol Psychiatry*
17. Xu H, Wang F, Liu Y, Yu Y, Gelernter J, Zhang H (2014) Sex-biased methylome and transcriptome in human prefrontal cortex. *Hum Mol Genet* 23(5):1260–1270
18. De Jager PL, Srivastava G, Lunnon K, Burgess J, Schalkwyk LC, Yu L, Eaton ML, Keenan BT, Ernst J, McCabe C, Tang A, Raj T, Replogle J, Brodeur W, Gabriel S, Chai HS, Younkin C, Younkin SG, Zou F, Szyf M, Epstein CB, Schneider JA, Bernstein BE, Meissner A, Ertekin-Taner N, Chibnik LB, Kellis M, Mill J, Bennett DA (2014) Alzheimer's disease: early alterations in brain DNA methylation at ANK1, BIN1, RHBDF2 and other loci. *Nat Neurosci* 17(9):1156–1163
19. Lunnon K, Smith R, Hannon E, De Jager PL, Srivastava G, Volta M, Troakes C, Al-Sarraj S, Burrage J, Macdonald R, Condliffe D, Harries LW, Katsel P, Haroutunian V, Kaminsky Z, Joachim C, Powell J, Lovestone S, Bennett DA, Schalkwyk LC, Mill J (2014) Methylomic profiling implicates cortical deregulation of ANK1 in Alzheimer's disease. *Nat Neurosci* 17(9):1164–1170
20. Smith RG, Hannon E, De Jager PL, Chibnik L, Lott SJ, Condliffe D, Smith AR, Haroutunian V, Troakes C, Al-Sarraj S, Bennett DA, Powell J, Lovestone S, Schalkwyk L, Mill J, Lunnon K (2018) Elevated DNA methylation across a 48-kb region spanning the HOXA gene cluster is associated with Alzheimer's disease neuropathology. *Alzheimer's Dementia* 14(12):1580–1588
21. Gasparoni G, Bultmann S, Lutsik P, Kraus T, Sordon S, Vlcek J, Dietinger V, Steinmaurer M, Haider M, Mulholland CB, Arzberger T, Roeder S, Riemenschneider M, Kretzschmar HA, Giese A, Leonhardt H, Walter J (2018) DNA methylation analysis on purified neurons and glia dissects age and Alzheimer's disease-specific changes in the human cortex. *Epigenetics Chromatin* 11(1):41
22. Zhang L, Silva TC, Young JI, Gomez L, Schmidt MA, Hamilton-Nelson KL, Kunkle BW, Chen X, Martin ER, Wang L (2020) Epigenome-wide meta-analysis of DNA methylation differences in prefrontal cortex implicates the immune processes in Alzheimer's disease. *Nat Commun* 11(1):6114
23. Ober C, Loisel DA, Gilad Y (2008) Sex-specific genetic architecture of human disease. *Nat Rev Genet* 9(12):911–922
24. Brookes ST, Whitely E, Egger M, Smith GD, Mulheran PA, Peters TJ (2004) Subgroup analyses in randomized trials: risks of subgroup-specific analyses; power and sample size for the interaction test. *J Clin Epidemiol* 57(3):229–236
25. Joehanes R, Just AC, Marioni RE, Pilling LC, Reynolds LM, Mandaviya PR, Guan W, Xu T, Elks CE, Aslibekyan S, Moreno-Macias H, Smith JA, Brody JA, Dhingra R, Yousefi P, Pankow JS, Kunze S, Shah SH, McRae AF, Lohman K, Sha J, Absher DM, Ferrucci L, Zhao W, Demerath EW, Bressler J, Grove ML, Huan T, Liu C, Mendelson MM, Yao C, Kiel DP, Peters A, Wang-Sattler R, Visscher PM, Wray NR, Starr JM, Ding J, Rodriguez CJ, Wareham NJ, Irvin MR, Zhi D, Barrdahl M, Vineis P, Ambatipudi S, Uitterlinden AG, Hofman A, Schwartz J, Colicino E, Hou L, Vokonas PS, Hernandez DG, Singleton AB, Bandinelli S, Turner ST, Ware EB, Smith AK, Klengel T, Binder EB, Psaty BM, Taylor KD, Gharib SA, Swenson BR, Liang L, DeMeo DL, O'Connor GT, Herceg Z, Ressler KJ, Conneely KN, Sotoodehnia N, Kardia SL, Melzer D, Baccarelli AA, van Meurs JB, Romieu I, Arnett DK, Ong KK, Liu Y, Waldenberger M, Deary IJ, Fornage M, Levy D, London SJ (2016) Epigenetic signatures of cigarette smoking. *Circ Cardiovasc Genet* 9(5):436–447
26. Wang T, Guan W, Lin J, Boutaoui N, Canino G, Luo J, Celedon JC, Chen W (2015) A systematic study of normalization methods for Infinium 450K methylation data using whole-genome bisulfite sequencing data. *Epigenetics* 10(7):662–669
27. Teschendorff AE, Marabita F, Lechner M, Bartlett T, Tegner J, Gomez-Cabrero D, Beck S (2013) A beta-mixture quantile normalization method for correcting probe design bias in Illumina Infinium 450 k DNA methylation data. *Bioinformatics* 29(2):189–196
28. Pidsley R, CC YW, Volta M, Lunnon K, Mill J, Schalkwyk LC (2013) A data-driven approach to preprocessing Illumina 450K methylation array data. *BMC Genomics* 14:293
29. Guintivano J, Aryee MJ, Kaminsky ZA (2013) A cell epigenotype specific model for the correction of brain cellular heterogeneity bias and its application to age, brain region and major depression. *Epigenetics* 8(3):290–302
30. Gomez L, Odom GJ, Young JI, Martin ER, Liu L, Chen X, Griswold AJ, Gao Z, Zhang L, Wang L (2019) coMethDMR: accurate identification of co-methylated and differentially methylated regions in epigenome-wide association studies with continuous phenotypes. *Nucleic Acids Res* 47(17):e98
31. Devlin B, Roeder K (1999) Genomic control for association studies. *Biometrics* 55(4):997–1004
32. van Iterson M, van Zwet EW, Consortium B, Heijmans BT (2017) Controlling bias and inflation in epigenome- and transcriptome-wide association studies using the empirical null distribution. *Genome Biol* 18(1):19
33. Higgins JP, Thompson SG (2002) Quantifying heterogeneity in a meta-analysis. *Stat Med* 21(11):1539–1558
34. Rice K, Higgins JLT (2018) A re-evaluation of fixed effect(s) meta-analysis. *J R Stat Soc A* 181:205–227
35. Riley RD, Higgins JP, Deeks JJ (2011) Interpretation of random effects meta-analyses. *BMJ* 342:d549
36. Van den Berge K, Sonesson C, Robinson MD, Clement L (2017) stageR: a general stage-wise method for controlling the gene-level false discovery rate in differential expression and differential transcript usage. *Genome Biol* 18(1):151
37. Chadwick LH (2012) The NIH Roadmap Epigenomics Program data resource. *Epigenomics* 4(3):317–324
38. Ernst J, Kellis M (2012) ChromHMM: automating chromatin-state discovery and characterization. *Nat Methods* 9(3):215–216
39. Yen A, Kellis M (2015) Systematic chromatin state comparison of epigenomes associated with diverse properties including sex and tissue type. *Nat Commun* 6:7973
40. Davis CA, Hitz BC, Sloan CA, Chan ET, Davidson JM, Gabdank I, Hilton JA, Jain K, Baymuradov UK, Narayanan AK, Onate KC, Graham K, Miyasato SR, Dreszer TR, Strattan JS, Jolanki O, Tanaka FY, Cherry JM (2018) The Encyclopedia of DNA elements (ENCODE): data portal update. *Nucleic Acids Res* 46(D1):D794–D801

41. Sanchez-Castillo M, Ruau D, Wilkinson AC, Ng FS, Hannah R, Diamanti E, Lombard P, Wilson NK, Gottgens B (2015) CODEX: a next-generation sequencing experiment database for the haematopoietic and embryonic stem cell communities. *Nucleic Acids Res* 43(Database issue):D1117–D1123
42. Sheffield NC, Bock C (2016) LOLA: enrichment analysis for genomic region sets and regulatory elements in R and Bioconductor. *Bioinformatics* 32(4):587–589
43. Subramanian A, Tamayo P, Mootha VK, Mukherjee S, Ebert BL, Gillette MA, Paulovich A, Pomeroy SL, Golub TR, Lander ES, Mesirov JP (2005) Gene set enrichment analysis: a knowledge-based approach for interpreting genome-wide expression profiles. *Proc Natl Acad Sci U S A* 102(43):15545–15550
44. McLean CY, Bristor D, Hiller M, Clarke SL, Schaar BT, Lowe CB, Wenger AM, Bejerano G (2010) GREAT improves functional interpretation of cis-regulatory regions. *Nat Biotechnol* 28(5):495–501
45. Wood SN (2001) mgcv: GAMs and Generalized Ridge Regression for R. *R News* 1(2):20–25
46. McCarthy S, Das S, Kretzschmar W, Delaneau O, Wood AR, Teumer A, Kang HM, Fuchsberger C, Danecek P, Sharp K, Luo Y, Sidore C, Kwong A, Timpson N, Koskinen S, Vrieze S, Scott LJ, Zhang H, Mahajan A, Veldink J, Peters U, Pato C, van Duijn CM, Gillies CE, Gandin I, Mezzavilla M, Gilly A, Cocca M, Traglia M, Angius A, Barrett JC, Boomsma D, Branham K, Breen G, Brummett CM, Busonero F, Campbell H, Chan A, Chen S, Chew E, Collins FS, Corbin LJ, Smith GD, Dedoussis G, Dorr M, Farmaki AE, Ferrucci L, Forer L, Fraser RM, Gabriel S, Levy S, Groop L, Harrison T, Hattersley A, Holmen OL, Hveem K, Kretzler M, Lee JC, McGue M, Meitinger T, Melzer D, Min JL, Mohlke KL, Vincent JB, Nauck M, Nickerson D, Palotie A, Pato M, Pirastu N, McInnis M, Richards JB, Sala C, Salomaa V, Schlessinger D, Schoenherr S, Slagboom PE, Small K, Spector T, Stambolian D, Tuke M, Tuomilehto J, Van den Berg LH, Van Rheenen W, Volker U, Wijmenga C, Toniolo D, Zeggini E, Gasparini P, Sampson MG, Wilson JF, Frayling T, de Bakker PI, Swertz MA, McCarrill S, Kooperberg C, Dekker A, Altshuler D, Willer C, Iacono W, Ripatti S, Soranzo N, Walter K, Swaroop A, Cucca F, Anderson CA, Myers RM, Boehnke M, McCarthy MI, Durbin R (2016) C. Haplotype Reference, A reference panel of 64,976 haplotypes for genotype imputation. *Nat Genet* 48(10):1279–1283
47. Hannon E, Dempster E, Viana J, Burrage J, Smith AR, Macdonald R, St Clair D, Mustard C, Breen G, Therman S, Kaprio J, Touloupoulou T, Hulshoff Pol HE, Bohlken MM, Kahn RS, Nenadic I, Hultman CM, Murray RM, Collier DA, Bass N, Gurling H, McQuillin A, Schalkwyk L, Mill J (2016) An integrated genetic-epigenetic analysis of schizophrenia: evidence for co-localization of genetic associations and differential DNA methylation. *Genome Biol* 17(1):176
48. Davies M, Nowotka M, Papadatos G, Dedman N, Gaulton A, Atkinson F, Bellis L, Overington JP (2015) ChEMBL web services: streamlining access to drug discovery data and utilities. *Nucleic Acids Res* 43(W1):W612–W620
49. Viana J, Hannon E, Dempster E, Pidsley R, Macdonald R, Knox O, Spiers H, Troakes C, Al-Saraj S, Turecki G, Schalkwyk LC, Mill J (2017) Schizophrenia-associated methylomic variation: molecular signatures of disease and polygenic risk burden across multiple brain regions. *Hum Mol Genet* 26(1):210–225
50. Prasad R, Jho EH (2019) A concise review of human brain methylation during aging and neurodegenerative diseases. *BMB Rep* 52(10):577–588
51. Heyn H, Li N, Ferreira HJ, Moran S, Pisano DG, Gomez A, Diez J, Sanchez-Mut JV, Setien F, Carmona FJ, Puca AA, Sayols S, Pujana MA, Serra-Musach J, Iglesias-Platas I, Formiga F, Fernandez AF, Fraga MF, Heath SC, Valencia A, Gut IG, Wang J, Esteller M (2012) Distinct DNA methylomes of newborns and centenarians. *Proc Natl Acad Sci U S A* 109(26):10522–10527
52. Reddington JP, Perricone SM, Nestor CE, Reichmann J, Youngson NA, Suzuki M, Reinhardt D, Dunican DS, Prendergast JG, Mjoseng H, Ramasahoye BH, Whitelaw E, Greally JM, Adams IR, Bickmore WA, Meehan RR (2013) Redistribution of H3K27me3 upon DNA hypomethylation results in de-repression of Polycomb target genes. *Genome Biol* 14(3):R25
53. Brinkman AB, Gu H, Bartels SJ, Zhang Y, Matarese F, Simmer F, Marks H, Bock C, Gnirke A, Meissner A, Stunnenberg HG (2012) Sequential ChIP-bisulfite sequencing enables direct genome-scale investigation of chromatin and DNA methylation cross-talk. *Genome Res* 22(6):1128–1138
54. von Schimmelmann M, Feinberg PA, Sullivan JM, Ku SM, Badimon A, Duff MK, Wang Z, Lachmann A, Dewell S, Ma'ayan A, Han MH, Tarakhovskiy A, Schaefer A (2016) Polycomb repressive complex 2 (PRC2) silences genes responsible for neurodegeneration. *Nat Neurosci* 19(10):1321–1330
55. GSEA/MSigDB Team, GSEA FAQ, 2020. https://software.broadinstitute.org/cancer/software/gsea/wiki/index.php/FAQ#Why_does_GSEA_use_a_false_discovery_rate_28FDR29_of_0.25_rather_than_the_more_classic_0.053F. Accessed 24 Nov 2020
56. Zhang B, Gaiteri C, Bodea LG, Wang Z, McElwee J, Podtelezchnikov AA, Zhang C, Xie T, Tran L, Dobrin R, Fluder E, Clurman B, Melquist S, Narayanan M, Suver C, Shah H, Mahajan M, Gillis T, Mysore J, MacDonald ME, Lamb JR, Bennett DA, Molony C, Stone DJ, Gudnason V, Myers AJ, Schadt EE, Neumann H, Zhu J, Emilsson V (2013) Integrated systems approach identifies genetic nodes and networks in late-onset Alzheimer's disease. *Cell* 153(3):707–720
57. Cosarderioglu C, Nidadavolu LS, George CJ, Oh ES, Bennett DA, Walston JD, Abadir PM (2020) Brain renin-angiotensin system at the intersect of physical and cognitive frailty. *Front Neurosci* 14:586314
58. Benigni A, Cassis P, Remuzzi G (2010) Angiotensin II revisited: new roles in inflammation, immunology and aging. *EMBO Mol Med* 2(7):247–257
59. Manoharan S, Guillemin GJ, Abiramandari RS, Essa MM, Akbar M, Akbar MD (2016) The role of reactive oxygen species in the pathogenesis of Alzheimer's disease. Parkinson's disease, and Huntington's disease: a mini review. *Oxid Med Cell Longev* 2016:8590578
60. Chen YY, Wang MC, Wang YN, Hu HH, Liu QQ, Liu HJ, Zhao YY (2020) Redox signaling and Alzheimer's disease: from pathomechanism insights to biomarker discovery and therapy strategy. *Biomark Res* 8:42
61. Rustenhoven J, Smith AM, Smyth LC, Jansson D, Scotter EL, Swanson MEV, Aalderink M, Coppieters N, Narayan P, Handley R, Overall C, Park TH, Schweder P, Heppner P, Curtis MA, Faull RLM, Dragunow M (2018) PU.1 regulates Alzheimer's disease-associated genes in primary human microglia. *Mol Neurodegener* 13(1):44
62. Deming Y, Dumitrescu L, Barnes LL, Thambisetty M, Kunkle B, Gifford KA, Bush WS, Chibnik LB, Mukherjee S, De Jager PL, Kukull W, Huentelman M, Crane PK, Resnick SM, Keene CD, Montine TJ, Schellenberg GD, Haines JL, Zetterberg H, Blennow K, Larson EB, Johnson SC, Albert M, Moghekar A, Del Aguila JL, Fernandez MV, Budde J, Hassentab J, Fagan AM, Riemenschneider M, Petersen RC, Minthon L, Chao MJ, Van Deerlin VM, Lee VM, Shaw LM, Trojanowski JQ, Peskind ER, Li G, Davis LK, Sealock JM, Cox NJ, Goate AM, Bennett DA, Schneider JA, Jefferson AL, Cruchaga C, Hohman TJ, I. Alzheimer's Disease Neuroimaging, C. Alzheimer Disease Genetics (2018) Sex-specific genetic predictors of Alzheimer's disease biomarkers. *Acta Neuropathol* 136(6):857–872
63. Dumitrescu L, Barnes LL, Thambisetty M, Beecham G, Kunkle B, Bush WS, Gifford KA, Chibnik LB, Mukherjee S, De Jager PL, Kukull W, Crane PK, Resnick SM, Keene CD, Montine TJ, Schellenberg GD, Deming Y, Chao MJ, Huentelman M, Martin ER, Hamilton-Nelson K, Shaw LM, Trojanowski JQ, Peskind ER, Cruchaga C, Pericak-Vance MA, Goate AM, Cox NJ, Haines JL, Zetterberg H, Blennow K, Larson EB, Johnson SC, Albert M, Bennett DA, Schneider JA, Jefferson AL, Hohman TJ, C. Alzheimer's Disease Neuroimaging, I. the Alzheimer's Disease Neuroimaging (2019) Sex differences in the genetic predictors of Alzheimer's pathology. *Brain* 142(9):2581–2589
64. Scacchi R, Gambina G, Broggio E, Corbo RM (2014) Sex and ESR1 genotype may influence the response to treatment with donepezil and rivastigmine in patients with Alzheimer's disease. *Int J Geriatr Psychiatry* 29(6):610–615
65. Ibarra M, Vazquez M, Fagiolino P, Derendorf H (2013) Sex related differences on valproic acid pharmacokinetics after oral single dose. *J Pharmacokinet Pharmacodyn* 40(4):479–486
66. ClinicalTrials.gov., Drug interaction study with a potential Alzheimer's disease compound. <https://clinicaltrials.gov/ct2/show/NCT00726726?id=%22NCT00692510%22OR%22NCT00726726%22&draw=2&rank=1>. Accessed 31 Jan 2021
67. ClinicalTrials.gov., Drug interaction study between AZD3480 and cytochrome P450 (Cocktail). <https://clinicaltrials.gov/ct2/show/NCT00692510?id=%22NCT00692510%22OR%22NCT00726726%22&draw=2&rank=2>. Accessed 31 Jan 2021

68. Driscoll I, Shumaker SA, Snively BM, Margolis KL, Manson JE, Vitolsins MZ, Rossom RC, Espeland MA (2016) Relationships between caffeine intake and risk for probable dementia or global cognitive impairment: the women's health initiative memory study. *J Gerontol A Biol Sci Med Sci* 71(12):1596–1602
69. Kim JW, Byun MS, Yi D, Lee JH, Jeon SY, Jung G, Lee HN, Sohn BK, Lee JY, Kim YK, Shin SA, Sohn CH, Lee DY, Group KR (2019) Coffee intake and decreased amyloid pathology in human brain. *Transl Psychiatry* 9(1):270
70. Jee HJ, Lee SG, Bormate KJ, Jung YS (2020) Effect of caffeine consumption on the risk for neurological and psychiatric disorders: sex differences in human. *Nutrients* 12(10):3080
71. Shimabukuro M, Jinno Y, Fuke C, Okazaki Y (2006) Haloperidol treatment induces tissue- and sex-specific changes in DNA methylation: a control study using rats. *Behav Brain Funct* 2:37
72. Shimabukuro M, Sasaki T, Imamura A, Tsujita T, Fuke C, Umekage T, Tochigi M, Hiramatsu K, Miyazaki T, Oda T, Sugimoto J, Jinno Y, Okazaki Y (2007) Global hypomethylation of peripheral leukocyte DNA in male patients with schizophrenia: a potential link between epigenetics and schizophrenia. *J Psychiatr Res* 41(12):1042–1046
73. Alfonso SI, Callender JA, Hooli B, Antal CE, Mullin K, Sherman MA, Lesne SE, Leitges M, Newton AC, Tanzi RE, Malinow R (2016) Gain-of-function mutations in protein kinase Calpha (PKCalpha) may promote synaptic defects in Alzheimer's disease. *Sci Signal* 9(427):ra47
74. John A, Reddy PH (2020) Synaptic basis of Alzheimer's disease: Focus on synaptic amyloid beta. P-tau and mitochondria. *Ageing Res Rev* 65:101208
75. Saura CA, Valero J (2011) The role of CREB signaling in Alzheimer's disease and other cognitive disorders. *Rev Neurosci* 22(2):153–169
76. DeKosky ST, Scheff SW (1990) Synapse loss in frontal cortex biopsies in Alzheimer's disease: correlation with cognitive severity. *Ann Neurol* 27(5):457–464
77. Terry RD, Masliah E, Salmon DP, Butters N, DeTeresa R, Hill R, Hansen LA, Katzman R (1991) Physical basis of cognitive alterations in Alzheimer's disease: synapse loss is the major correlate of cognitive impairment. *Ann Neurol* 30(4):572–580
78. Masliah E, Mallory M, Alford M, DeTeresa R, Hansen LA, McKeel DW Jr, Morris JC (2001) Altered expression of synaptic proteins occurs early during progression of Alzheimer's disease. *Neurology* 56(1):127–129
79. Scheff SW, Price DA, Schmitt FA, DeKosky ST, Mufson EJ (2007) Synaptic alterations in CA1 in mild Alzheimer disease and mild cognitive impairment. *Neurology* 68(18):1501–1508
80. C. International Multiple Sclerosis Genetics (2010) Comprehensive follow-up of the first genome-wide association study of multiple sclerosis identifies KIF21B and TMEM39A as susceptibility loci. *Hum Mol Genet* 19(5): 953–962
81. Varade J, Comabella M, Ortiz MA, Arroyo R, Fernandez O, Pinto-Medel MJ, Fedetz M, Izquierdo G, Lucas M, Gomez CL, Rabasa AC, Alcina A, Matesanz F, Alloza I, Antiguedad A, Garcia-Barcina M, Otaegui D, Olascoaga J, Saiz A, Blanco Y, Montalban X, Vandenbroeck K, Urcelay E (2012) Replication study of 10 genes showing evidence for association with multiple sclerosis: validation of TMEM39A, IL12B and CBLB [correction of CLBL] genes. *Mult Scler* 18(7):959–965
82. Tran Q, Park J, Lee H, Hong Y, Hong S, Park S, Park J, Kim SH (2017) TMEM39A and human diseases: a brief review. *Toxicol Res* 33(3):205–209
83. Ferrer-Ferrer M, Dityatev A (2018) Shaping synapses by the neural extracellular matrix. *Front Neuroanat* 12:40
84. Kunkle BW, Grenier-Boley B, Sims R, Bis JC, Damotte V, Naj AC, Boland A, Vronskaya M, van der Lee SJ, Amalie-Wolf A, Bellenguez C, Frizatti A, Chouraki V, Martin ER, Sleegers K, Badarinarayan N, Jakobsdottir J, Hamilton-Nelson KL, Moreno-Grau S, Ojano R, Raybould R, Chen Y, Kuzma AB, Hiltunen M, Morgan T, Ahmad S, Vardarajan BN, Epelbaum J, Hoffmann P, Boada M, Beecham GW, Garnier JG, Harold D, Fitzpatrick AL, Valladares O, Moutet ML, Gerrish A, Smith AV, Qu L, Bacq D, Denning N, Jian X, Zhao Y, Del Zompo M, Fox NC, Choi SH, Mateo I, Hughes JT, Adams HH, Malamon J, Sanchez-Garcia F, Patel Y, Brody JA, Dombroski BA, Naranjo MCD, Daniilidou M, Eiriksdottir G, Mukherjee S, Wallon D, Uphill J, Aspelund T, Cantwell LB, Garzía F, Galimberti D, Hofer E, Butkiewicz M, Fin B, Scarpini E, Sarnowski C, Bush WS, Meslage S, Kornhuber J, White CC, Song Y, Barber RC, Engelborghs S, Sordon S, Vojnovic D, Adams PM, Vandenbergh R, Mayhaus M, Cupples LA, Albert MS, De Deyn PP, Gu W, Himali JJ, Beekly D, Squassina A, Hartmann AM, Orellana A, Blacker D, Rodriguez-Rodriguez E, Lovestone S, Garcia ME, Doody RS, Munoz-Fernandez C, Sussams R, Lin H, Fairchild TJ, Benito YA, Holmes C, Karamujic-Comic H, Frosch MP, Thonberg H, Maier W, Roshchupkin G, Ghetti B, Giedraitis V, Kawalia A, Li S, Huebinger RM, Kilander L, Moebus S, Hernandez I, Kamboh MI, Brundin R, Turton J, Yang Q, Katz MJ, Concari L, Lord J, Beiser AS, Keene CD, Helisalmi S, Kloszewska I, Kukull WA, Koivisto AM, Lynch A, Tarraga L, Larson EB, Haapasalo A, Lawlor B, Mosley TH, Lipton RB, Solfrizzi V, Gill M, Longstreth WT Jr, Montine TJ, Frisardi V, Diez-Fairen M, Rivadeneira F, Petersen RC, Deramecourt V, Alvarez I, Salani F, Ciaramella A, Boerwinkle E, Reiman EM, Fievet N, Rotter JI, Reich JS, Hanon O, Cupidi C, Andre Uitterlinden AG, Royall DR, Dufouil C, Maletta RG, de Rojas I, Sano M, Brice A, Cecchetti R, George-Hyslop PS, Ritchie K, Tsalaki M, Tsuang DW, Dubois B, Craig D, Wu CK, Soininen H, Avramidou D, Albin RL, Fratiglioni L, Germanou A, Apostolova LG, Keller L, Koutroumani M, Arnold SE, Panza F, Gkatzima O, Asthana S, Hannequin D, Whitehead P, Atwood CS, Caffarra P, Hampel H, Quintela I, Carracedo A, Lannfelt L, Rubinsztein DC, Barnes LL, Pasquier F, Frolich L, Barral S, McGuinness B, Beach TG, Johnston JA, Becker JT, Passmore P, Bigio EH, Schott JM, Bird TD, Warren JD, Boeve BF, Lupton MK, Bowen JD, Proitsi P, Boxer A, Powell JF, Burke JR, Kauwe JSK, Burns JM, Mancuso M, Buxbaum JD, Bonuccelli U, Cairns NJ, McQuillin A, Cao C, Livingston G, Carlson CS, Bass NJ, Carlsson CM, Hardy J, Carney RM, Bras J, Carrasquillo MM, Guerreiro R, Allen M, Chui HC, Fisher E, Masullo C, Crocco EA, DeCarli C, Bisceglia G, Dick M, Ma L, Duara R, Graff-Radford NR, Evans DA, Hodges A, Faber KM, Scherer M, Fallon KB, Riemenschneider M, Fardo DW, Heun R, Farlow MR, Kolsch H, Ferris S, Leber M, Foroud TM, Heuser I, Galasko DR, Giegling I, Gearing M, Hull M, Geschwind DH, Gilbert JR, Morris J, Green RC, Mayo K, Growdon JH, Feulner T, Hamilton RL, Harrell LE, Driche D, Honig LS, Cushion TD, Huentelman MJ, Hollingworth P, Hulette CM, Hyman BT, Marshall R, Jarvik GP, Meggy A, Abner E, Menzies GE, Jin LW, Leonenko G, Real LM, Jun GR, Baldwin CT, Grozeva D, Karydas A, Russo G, Kaye JA, Kim R, Jessen F, Kowall NW, Vellas B, Kramer JH, Vardy E, LaFerla FM, Jockel KH, Lah JJ, Dichgans M, Leverenz JB, Mann D, Levey AI, Pickering-Brown S, Lieberman AP, Klopp N, Lunetta KL, Wichmann HE, Lyketsos CG, Morgan K, Marson DC, Brown K, Martiniuk F, Medway C, Mash DC, Nothen MM, Masliah E, Hooper NM, McCormick WC, Daniele A, McCurry SM, Bayer A, McDavid AN, Gallacher J, McKee AC, van den Bussche H, Mesulam M, Brayne C, Miller BL, Riedel-Heller S, Miller CA, Miller JW, Al-Chalabi A, Morris JC, Shaw CE, Myers AJ, Wiltfang J, O'Bryant S, Olichney JM, Alvarez V, Parisi JE, Singleton AB, Paulson HL, Collinge J, Perry WR, Mead S, Peskind E, Cribbs DH, Rossor M, Pierce A, Ryan NS, Poon WW, Nacmias B, Potter H, Sorbi S, Quinn JF, Sacchinelli E, Raj A, Spalletta G, Raskind M, Caltagirone C, Bossu P, Orfei MD, Reisberg B, Clarke R, Reitz C, Smith AD, Ringman JM, Warden D, Roberson ED, Wilcock G, Rogaeva E, Bruni AC, Rosen HJ, Gallo M, Rosenberg RN, Ben-Shlomo Y, Sager MA, Mecocci P, Saykin AJ, Pastor P, Cuccaro ML, Vance JM, Schneider JA, Schneider LS, Slifer S, Seeley WW, Smith AG, Sonnen JA, Spina S, Stern RA, Swerdlow RH, Tang M, Tanzi RE, Trojanowski JQ, Troncoso JC, Van Deerlin VM, Van Eldik LJ, Vinters HV, Vonsattel JP, Weintraub S, Welsh-Bohmer KA, Wilhelmson KC, Williamson J, Wingo TS, Woltjer RL, Wright CB, Yu CE, Yu L, Saba Y, Pilotto A, Bullido MJ, Peters O, Crane PK, Bennett D, Bosco P, Coto E, Boccardi V, De Jager PL, Lleo A, Warner N, Lopez OL, Ingelsson M, Deloukas P, Cruchaga C, Graff C, Gwilliam R, Fornage M, Goate AM, Sanchez-Juan P, Kehoe PG, Amin N, Ertekin-Taner N, Berr C, Debette S, Love S, Launer LJ, Younkin SG, Dartigues JF, Corcoran C, Ikram MA, Dickson DW, Nicolas G, Campion D, Tschanz J, Schmidt H, Hakonarson H, Clarimon J, Munger R, Schmidt R, Farrer LA, Van Broeckhoven C, M COD, DeStefano AL, Jones L, Haines JL, Deleuze JF, Owen MJ, Gudnason V, Mayeux R, Escott-Price V, Psaty BM, Ramirez A, Wang LS, Ruiz A, van Duijn CM, Holmans PA, Seshadri S, Williams J, Amouyel P, Schellenberg GD, Lambert JC, Pericak-Vance MA, C. Alzheimer Disease Genetics, I. European Alzheimer's Disease, H. Cohorts for, C. Aging Research in Genomic Epidemiology, Genetic, P. Environmental Risk in Ad/Defining Genetic, C. Environmental Risk for Alzheimer's Disease (2019) Genetic meta-analysis of diagnosed Alzheimer's disease identifies new risk loci and implicates Abeta, tau, immunity and lipid processing. *Nat Genet* 51(3):414–430

85. Ramasamy A, Trabzuni D, Guelfi S, Varghese V, Smith C, Walker R, De T, Coin L, de Silva R, Cookson MR, Singleton AB, Hardy J, Ryten M, Weale ME, U.K.B.E. Consortium, C. North American Brain Expression (2014) Genetic variability in the regulation of gene expression in ten regions of the human brain. *Nat Neurosci* 17(10):1418–1428
86. Watson CT, Roussos P, Garg P, Ho DJ, Azam N, Katsel PL, Haroutunian V, Sharp AJ (2016) Genome-wide DNA methylation profiling in the superior temporal gyrus reveals epigenetic signatures associated with Alzheimer's disease. *Genome Med* 8(1):5
87. Bakulski KM, Dolinoy DC, Sartor MA, Paulson HL, Konen JR, Lieberman AP, Albin RL, Hu H, Rozek LS (2012) Genome-wide DNA methylation differences between late-onset Alzheimer's disease and cognitively normal controls in human frontal cortex. *J Alzheimers Dis* 29(3):571–588
88. Spiers H, Hannon E, Schalkwyk LC, Smith R, Wong CC, O'Donovan MC, Bray NJ, Mill J (2015) Methylomic trajectories across human fetal brain development. *Genome Res* 25(3):338–352
89. Perzel Mandell KA, Price AJ, Wilton R, Collado-Torres L, Tao R, Eagles NJ, Szalay AS, Hyde TM, Weinberger DR, Kleinman JE, Jaffe AE (2021) Characterizing the dynamic and functional DNA methylation landscape in the developing human cortex. *Epigenetics* 16(1):1–3
90. Ma J, Jiang T, Tan L, Yu JT (2015) TYROBP in Alzheimer's disease. *Mol Neurobiol* 51(2):820–826
91. Pottier C, Ravenscroft TA, Brown PH, Finch NA, Baker M, Parsons M, Asmann YW, Ren Y, Christopher E, Levitch D, van Blitterswijk M, Cruchaga C, Campion D, Nicolas G, Richard AC, Guerreiro R, Bras JT, Zuchner S, Gonzalez MA, Bu G, Younkin S, Knopman DS, Josephs KA, Parisi JE, Petersen RC, Ertekin-Taner N, Graff-Radford NR, Boeve BF, Dickson DW, Rademakers R (2016) TYROBP genetic variants in early-onset Alzheimer's disease. *Neurobiol Aging* 48:2229–22215
92. Paloneva J, Manninen T, Christman G, Hovanec K, Mandelin J, Adolfsson R, Bianchin M, Bird T, Miranda R, Salmaggi A, Tranebjaerg L, Konttinen Y, Peltonen L (2002) Mutations in two genes encoding different subunits of a receptor signaling complex result in an identical disease phenotype. *Am J Hum Genet* 71(3):656–662
93. Huang KL, Marcora E, Pimenova AA, Di Narzo AF, Kapoor M, Jin SC, Harari O, Bertelsen S, Fairfax BP, Czajkowski J, Chouraki V, Grenier-Boley B, Bellenguez C, Deming Y, McKenzie A, Raj T, Renton AE, Budde J, Smith A, Fitzpatrick A, Bis JC, DeStefano A, Adams HHH, Ikram MA, van der Lee S, Del-Aguila JL, Fernandez MV, Ibanez L, Sims R, Escott-Price V, Mayeux R, Haines JL, Farrer LA, Pericak-Vance MA, Lambert JC, van Duijn C, Launer L, Seshadri S, Williams J, Amouyel P, Schellenberg GD, Zhang B, Borecki I, Kauwe JSK, Cruchaga C, Hao K, Goate AM, P. International Genomics of Alzheimer's, I. Alzheimer's Disease Neuroimaging (2017) A common haplotype lowers PU1 expression in myeloid cells and delays onset of Alzheimer's disease. *Nat Neurosci* 20(8):1052–1061
94. Sessa G, Podini P, Mariani M, Meroni A, Spreafico R, Sinigaglia F, Colonna M, Panina P, Meldolesi J (2004) Distribution and signaling of TREM2/DAP12, the receptor system mutated in human polycystic lipomembraneous osteodysplasia with sclerosing leukoencephalopathy dementia. *Eur J Neurosci* 20(10):2617–2628
95. Bjorkqvist M, Ohlsson M, Minthon L, Hansson O (2012) Evaluation of a previously suggested plasma biomarker panel to identify Alzheimer's disease. *PLoS ONE* 7(1):e29868
96. Ray S, Britschgi M, Herbert C, Takeda-Uchimura Y, Boxer A, Blennow K, Friedman LF, Galasko DR, Jutel M, Karydas A, Kaye JA, Leszek J, Miller BL, Minthon L, Quinn JF, Rabinovici GD, Robinson WH, Sabbagh MN, So YT, Sparks DL, Tabaton M, Tinklenberg J, Yesavage JA, Tishirani R, Wyss-Coray T (2007) Classification and prediction of clinical Alzheimer's diagnosis based on plasma signaling proteins. *Nat Med* 13(11):1359–1362
97. Morgan BP (2018) Complement in the pathogenesis of Alzheimer's disease. *Semin Immunopathol* 40(1):113–124
98. Wennstrom M, Nielsen HM (2012) Cell adhesion molecules in Alzheimer's disease. *Degener Neurol Neuromuscul Dis* 2:65–77
99. Sil S, Periyasamy P, Thangaraj A, Chivero ET, Buch S (2018) PDGF/PDGFR axis in the neural systems. *Mol Aspects Med* 62:63–74
100. Jha NK, Jha SK, Kar R, Nand P, Swati K, Goswami VK (2019) Nuclear factor-kappa beta as a therapeutic target for Alzheimer's disease. *J Neurochem* 150(2):113–137
101. B. Qin, L. Li, S. Wang, J. Wu, Y. Huang, P. Zhou, J. Bai, Y. Zheng, Interleukin-8 gene polymorphism -251T>A contributes to Alzheimer's disease susceptibility. *Medicine (Baltimore)* 95(39) (2016) e5039.
102. Bacher M, Deuster O, Aljabari B, Egensperger R, Neff F, Jessen F, Popp J, Noelker C, Reese JP, Al-Abed Y, Dodel R (2010) The role of macrophage migration inhibitory factor in Alzheimer's disease. *Mol Med* 16(3–4):116–121
103. Fiebich BL, Batista CRA, Saliba SW, Yousif NM, de Oliveira ACP (2018) Role of microglia TLRs in neurodegeneration. *Front Cell Neurosci* 12:329
104. Chang R, Yee KL, Sumbria RK (2017) Tumor necrosis factor alpha Inhibition for Alzheimer's disease. *J Cent Nerv Syst Dis* 9:1179573517709278
105. Armato U, Chakravarthy B, Pacchiana R, Whitfield JF (2013) Alzheimer's disease: an update of the roles of receptors, astrocytes and primary cilia (review). *Int J Mol Med* 31(1):3–10
106. Ono K, Yamada M (2012) Vitamin A and Alzheimer's disease. *Geriatr Gerontol Int* 12(2):180–188
107. Kanaan NM, Piginio GF, Brady ST, Lazarov O, Binder LI, Morfini GA (2013) Axonal degeneration in Alzheimer's disease: when signaling abnormalities meet the axonal transport system. *Exp Neurol* 246:44–53
108. Schettters STT, Gomez-Nicola D, Garcia-Vallejo JJ, Van Kooyk Y (2017) Neuroinflammation: microglia and T cells get ready to tango. *Front Immunol* 8:1905
109. Esposito M, Sherr GL (2019) Epigenetic modifications in Alzheimer's neuropathology and therapeutics. *Front Neurosci* 13:476
110. Griffin JW, Bradshaw PC (2017) Amino acid catabolism in Alzheimer's disease brain: friend or foe? *Oxid Med Cell Longev* 2017:5472792
111. Conway ME (2020) Alzheimer's disease: targeting the glutamatergic system. *Biogerontology* 21(3):257–274

Publisher's Note

Springer Nature remains neutral with regard to jurisdictional claims in published maps and institutional affiliations.

Ready to submit your research? Choose BMC and benefit from:

- fast, convenient online submission
- thorough peer review by experienced researchers in your field
- rapid publication on acceptance
- support for research data, including large and complex data types
- gold Open Access which fosters wider collaboration and increased citations
- maximum visibility for your research: over 100M website views per year

At BMC, research is always in progress.

Learn more biomedcentral.com/submissions

